

CHAPTER-3

Effect of Ylide Substitution on the Stability and Electron Donation Ability of NHCs

Abstract: The first part of this chapter deals with the study of the effect of ylide substitution on the stability and σ -donating ability of a number of cyclic carbenes. The stabilities of all of the carbenes were investigated from an evaluation of their singlet–triplet energy gaps and stabilization energies. The energy of the σ -symmetric lone-pair orbital at the C_C atom increases as a result of the introduction of ylide centers near to the C_C atom. This indicates an enhanced σ -donating ability of the ylide-containing carbenes.

In the second part of this chapter, we made an attempt toward increasing the singlet state stability of remote *N*-heterocyclic carbenes. Theoretical investigations predict that the singlet states of ylide-substituted remote carbenes are significantly stable and comparable to those of experimentally known NHCs. They are also found to be strongly σ -donating in nature. NICS and QTAIM based bond magnetizability calculations indicate the presence of cyclic electron delocalization in majority of the molecules.

[3.1] Moving Toward Ylide–Stabilized Carbenes

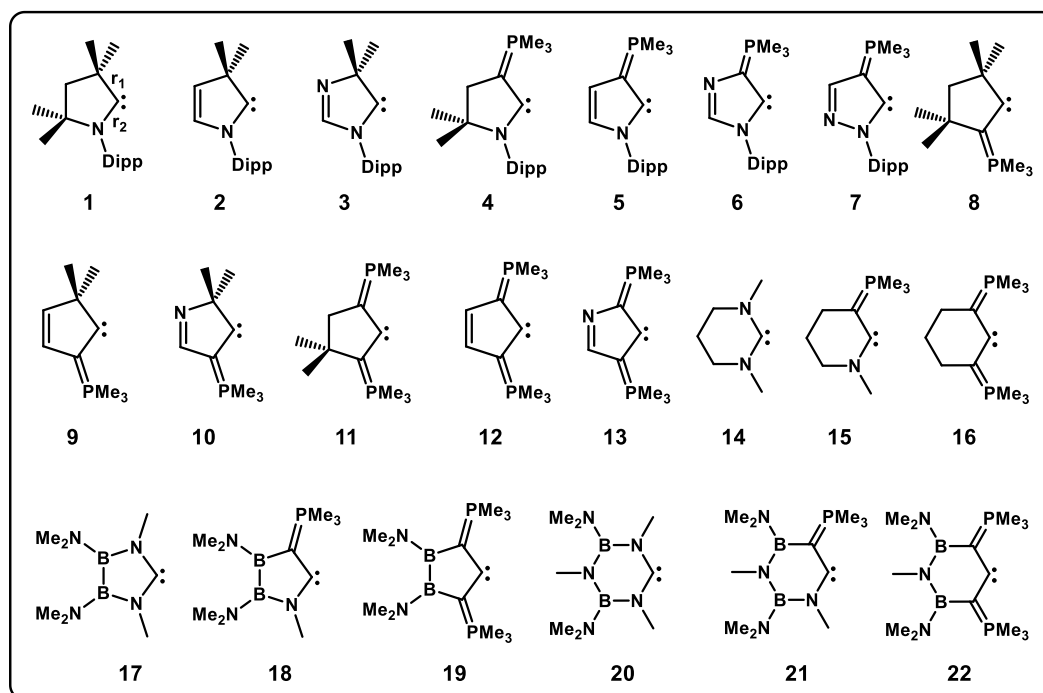
[3.1.1] Introduction

The neutral divalent species carbene can exhibit two spin states that depend on the nature of occupancy of the two nonbonding electrons. A singlet state arises if the two nonbonding electrons reside within the same orbital with anti-parallel spin, whereas two nonbonding electrons residing in two mutually perpendicular orbitals with parallel spin give rise to a triplet state. The parent carbene (:CH₂) possesses a triplet ground state [1], but carbenes with stable singlet states have also been reported. A signature example of a carbene with a stable singlet state is the *N*-heterocyclic carbene (NHC) [2], these have been widely used for more than two decades in many organic transformations and transition-metal-mediated catalysis [3–8]. The remarkable stability of the singlet state of NHCs is traced to the extensive π donation from the lone pairs of the neighboring nitrogen atoms (N_{LP}) to the formally vacant p orbital of the carbene center ($N_{LP} \rightarrow C_{P\pi}$) [9]. The stronger the $N_{LP} \rightarrow C_{P\pi}$ interaction is, the higher the stability of the singlet state will be. Thus, the presence of a heteroatom next to the carbene center was considered as a necessary criterion for obtaining stable singlet carbenes. On this basis, six years after the isolation of NHCs, a new class of isolable cyclic carbenes, the thiazolyliidenes, was prepared with nitrogen and sulfur atoms as the heteroatoms [10]. Similarly, in 2005, a P-heterocyclic carbene (PHC) was isolated [11]. However, the singlet–triplet separations of the thiazolyliidenes and the PHC were found to be lower than those of NHCs [12]. This difference in the singlet–triplet separations arises from the inferior π -donating ability of sulfur and phosphorus relative to that of nitrogen. However, the isolation of a cyclopropenyliene derivative by Bertrand and co-workers indicated the possibility of a stable cyclic carbene without the presence of a heteroatom directly bonded to the carbene center [13].

NHCs have been found to have very good σ -donating ability, as well as considerable π -accepting ability [14,15]. The enhanced σ -donating ability and steric bulk of NHCs allows them to replace phosphines as the ligands in many transition-metal catalysts, like the Grubbs second-generation olefin-metathesis catalyst [16,17]. In 2005, Bertrand and co-workers isolated a cyclic(alkyl)(amino)carbene (CAAC), which possesses better σ basicity and π acidity than the NHCs [18,19]. The Pd^{II} and Au^I complexes of CAAC have shown surprising and novel catalytic behavior [20,21]. The more nucleophilic and electrophilic character of CAAC was found to be advantageous in

the activation of small molecules like H₂, NH₃ and P₄ [22, 23]. This has opened up a new possibility for the design of stable singlet carbenes with better σ -donating ability.

The electron-donating ability of the carbene ligand has a significant effect on the catalytic activity of the corresponding transition-metal complexes. Hence, the design and synthesis of carbene frameworks with enhanced electron-donating abilities may help to develop novel catalysts for various applications. One way to enhance the σ basicity of carbenes is by skeletal substitution or placement of appropriate substituents at the atoms adjacent to the carbene center. Another way is to introduce electron-donating phosphorus and sulfur ylide centers into the ring framework [24]. The installation of ylide centers next to the carbenic carbon atom is expected not only to enhance the σ -donating ability but also to stabilize the carbene molecule. The enhanced σ -donating ability results from a smaller inductive effect of the ylide groups relative to the amino groups, whereas the stabilization comes from effective π donation of the ylide carbanion to the carbene center. To the best of our knowledge, apart from the seminal works of Kawashima and Fürstner in 2008 [24], there has been no systematic study, either theoretical or experimental, toward the exploration of this novel class of ylide-stabilized carbenes. In this work, we make an effort towards contributing to the field of phosphorus ylide stabilized carbenes (Scheme 3.1.1). It was found previously that the electron-donating



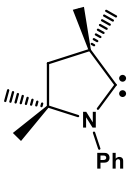
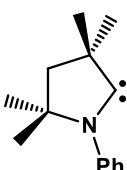
Scheme 3.1.1: Schematic representation of the range of carbenes considered in this study (Dipp: 2,6-diisopropylphenyl) [25].

abilities of sulfur ylide stabilized carbenes are lower than those with phosphorus ylide substitution [24c], so we did not consider sulfur ylide stabilized carbenes in the present study. We have considered both five- and six-membered parent carbenes, as well as their skeletally substituted derivatives, to understand the effect of ylide substitution on the electron-donating ability and stability. Furthermore, this study also includes hitherto-unknown ylide-stabilized boron substituted carbenes.

[3.1.2] Computational Details

Density functional theory calculations were performed to optimize all of the molecules with the hybrid PBE0 exchange-correlation functional [26]. We used the 6-31+G* basis set for main group elements and the SDD basis set with the Stuttgart–Dresden relativistic effective core potential for the rhodium atom [27]. To check the reliability of the basis set and the functional, the singlet–triplet separation of a representative molecule was evaluated by employing four different basis sets and functional (Table 3.1.1).

Table 3.1.1: Comparison of the singlet-triplet gaps (ΔE_{S-T} , in kcal mol⁻¹) using different basis sets and functionals.

Molecule	Functional/Basis set	ΔE_{S-T}
	BP86/6-31+G*	40.7
	BP86/6-311+G**	40.4
	BP86/TZVP	40.5
	BP86/aug-cc-pVTZ	39.8
	BP86/6-31+G*	40.7
	B3LYP/6-31+G*	42.7
	PBE0/6-31+G*	39.2
	TPSSH/6-31+G*	38.6
	M06/6-31+G*	42.8

It is evident from Table 3.1.1 that there is no appreciable change in the values of the singlet–triplet energy gaps (ΔE_{S-T}), which indicates that the basis set and the functional used in our study were quite adequate to predict the singlet–triplet gap and other properties considered in this study. This level of theory was found to be adequate in dealing with similar systems, as reported recently [28,29]. Furthermore, we have

calculated the ^{13}C NMR chemical shifts of the experimentally known molecules (**1**, **14**, **17** and **20**) and found that the level of theory used in this work could successfully reproduce the observed NMR shifts (Table 3.1.2). Frequency calculations were

Table 3.1.2: Comparison of the calculated and observed ^{13}C NMR chemical shifts (ppm) of experimentally known molecules.

Molecule	^{13}C Chemical Shifts (Calculated)	^{13}C Chemical Shifts (Observed)	Ref
1	320.4	304–319	[18]
14	228.8	244.5–245.1 ^a	[30]
17	298.6	304	[31]
20	275.7	281.6–282.9	[32]

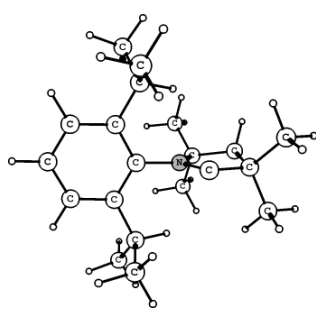
^aThe larger discrepancy between the calculated and observed chemical shifts for **14** may arise from the fact that while the calculations were carried by considering CH_3 as the substituent at the N atom, the actual molecule contains bulky aromatic xylyl or mesityl as the substituents.

performed at the same level of theory to characterize the nature of the stationary point. All structures were found to be minima on the potential energy surface with real frequencies. Natural-bonding analyses were performed with the natural-bond-orbital (NBO) partitioning scheme [33], as implemented in the Gaussian 03 suite of programs [34]. We calculated the nucleophilicity index with reference to tetracyanoethylene (TCNE), which was optimized at the same level of theory.

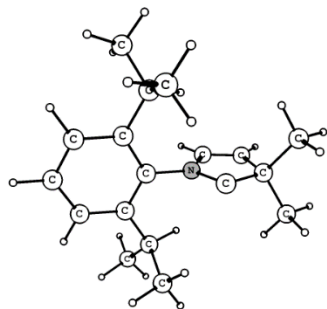
[3.1.3] Results and Discussion

[3.1.3.1] Molecular Geometries

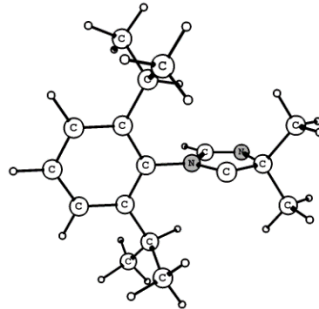
The central rings of **2**, **3**, **5–7**, **9**, **10**, **12**, **13** and **20–22** are found to have a perfectly planar structure in the optimized stable singlet state and a slightly distorted structure for others (Figure 3.1.1). The important geometrical parameters of **1–22** in the singlet state are listed in Table 3.1.3. All of the carbene molecules (except **11**) have a wider $\text{E}-\text{C}_\text{C}-\text{E}$ (C_C : central carbenic carbon atom; E: C or N) bond angle in the triplet state than in the singlet state. Two different $\text{C}_\text{C}-\text{E}$ bond lengths are obtained for the molecules with an unsymmetrical skeleton. Our calculated $\text{C}_\text{C}-\text{E}$ bond lengths and $\text{E}-\text{C}_\text{C}-\text{E}$ bond angles for **1**, **14**, **17** and **20** are in excellent agreement with the experimentally observed values (Table 3.1.3). A comparison of the geometrical parameters of **1–3** indicates that there is a significant change in the central $\text{E}-\text{C}_\text{C}-\text{E}$ bond



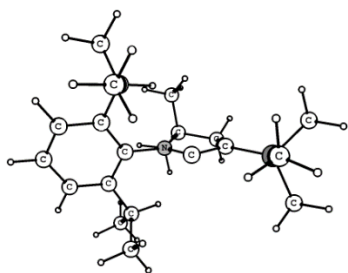
1



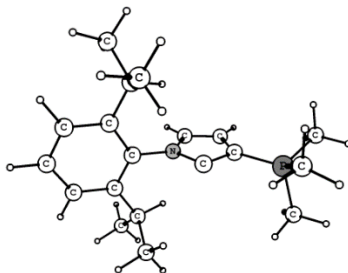
2



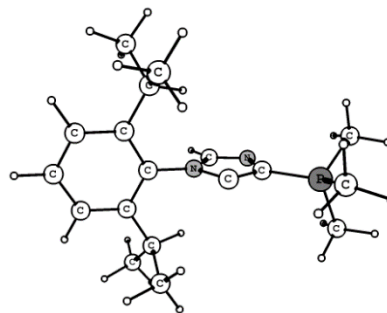
3



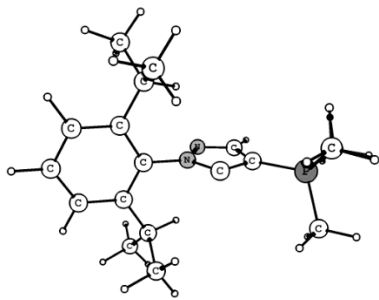
4



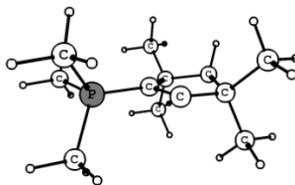
5



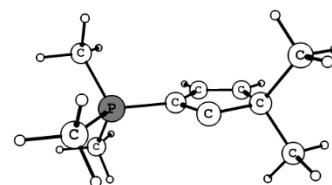
6



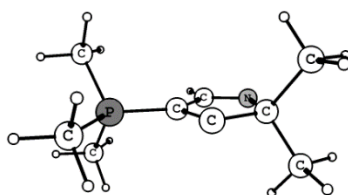
7



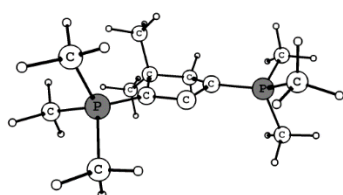
8



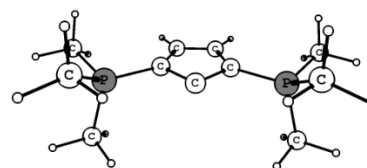
9



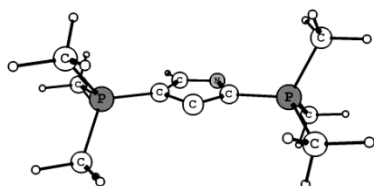
10



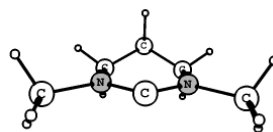
11



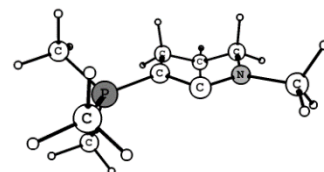
12



13



14



15

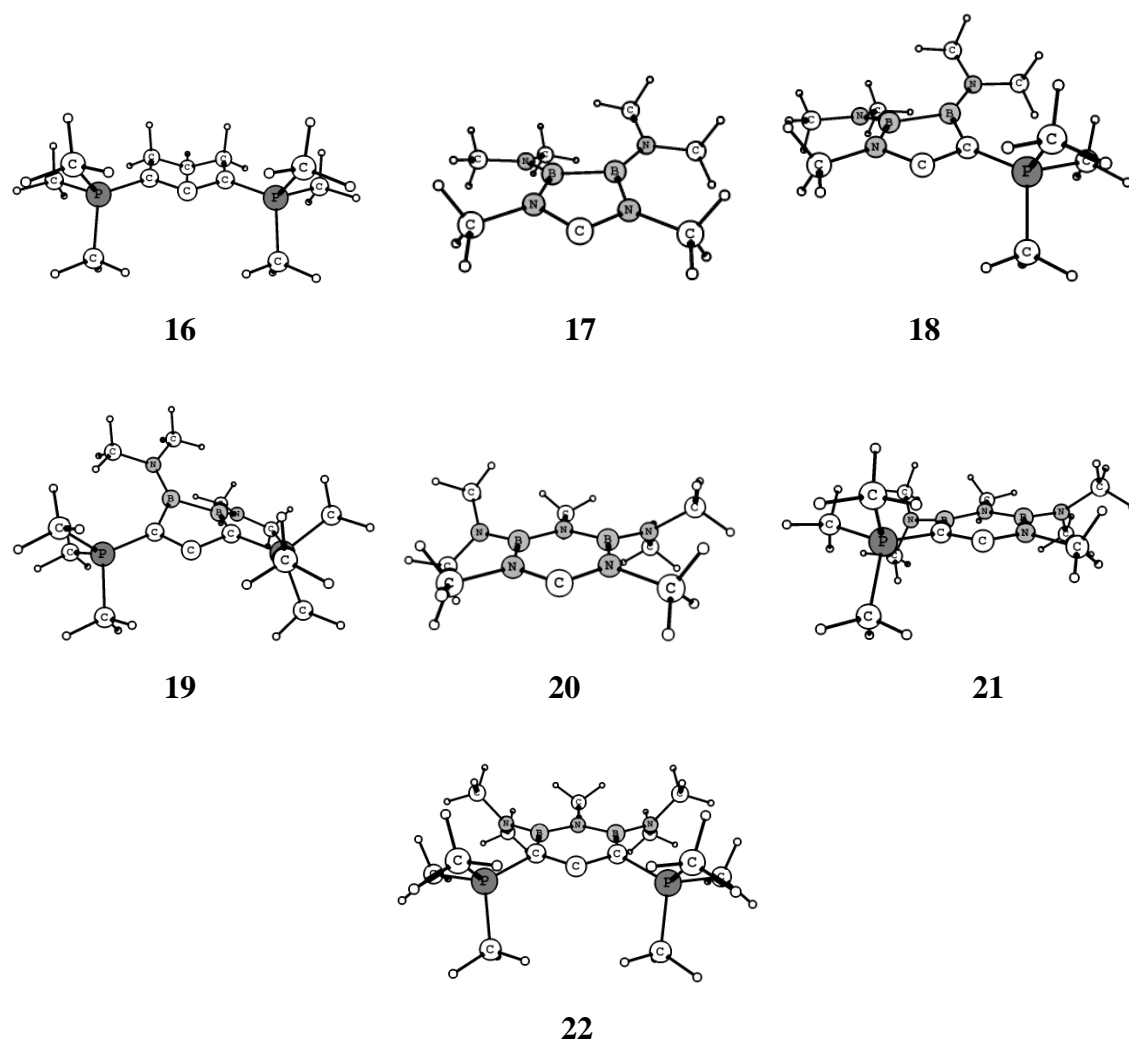


Figure 3.1.1: Optimized singlet state geometries of all the carbenes (1–22).

angle as a result of changes in the backbone of the ring framework. There is also a marginal change in the C_C –E bond lengths. Similar results are obtained for 4–6, 8–10 and 11–13. Replacement of the two methyl groups attached to the carbon atom in α position to the C_C atom in 1–3 by the ylide centers in 4–7 changes the C_C –E bond lengths significantly. The C_C –C (r_1) bond lengths are found to decrease, whereas there is an increase in the C_C –N (r_2) bond lengths. This indicates an increase in electron delocalization between the formally vacant p orbital of the C_C atom and the adjacent carbon atom (C_α) but a decrease in delocalization from the nitrogen lone pair (N_{LP}) to the formally vacant p orbital of the C_C atom. This is also evident from the increase in occupancy of the N_{LP} in 4–7 (1.682, 1.578, 1.572 and 1.561, respectively) relative to that in 1–3 (1.551, 1.540 and 1.542, respectively). The E– C_C –E bond angles also change appreciably. There is an increase in the C_C –E (both r_1 and r_2) bond lengths and a slight

Table 3.1.3: PBE0/6-31+G* calculated C_C-E bond lengths (r_1/r_2 in Å) and E-C_C-E bond angles (in degrees) in the singlet state geometry of **1–22** (where E = C or N). Experimental values are given within parenthesis.

Molecule	r_1/r_2	$\angle\text{E-C}_\text{C}\text{-E}$	Ref.
1	1.519/1.311 (1.516/1.315)	106.3 (106.5)	[18]
2	1.524/1.325	103.6	
3	1.515/1.326	101.8	
4	1.405/1.359	105.2	
5	1.419/1.375	101.2	
6	1.404/1.387	98.3	
7	1.422/1.355	99.9	
8	1.529/1.362	105.0	
9	1.533/1.380	102.5	
10	1.522/1.380	100.6	
11	1.414/1.415	104.0	
12	1.425/1.425	99.9	
13	1.409/1.433	97.1	
14	1.345/1.345 (1.346)	115.6 (114.6)	[30]
15	1.401/1.350	116.0	
16	1.404/1.404	116.3	
17	1.371/1.371 (1.352/1.404)	110.8 (108.4)	[31]
18	1.429/1.376	112.4	
19	1.439/1.439	111.5	
20	1.360/1.360 (1.366/1.363)	114.9 (114.4)	[32]
21	1.408/1.368	115.4	
22	1.418/1.418	115.7	

decrease in the E-C_C-E bond angles upon replacement of the amino groups of **1–3** with the ylide centers in **8–10**. However, molecules **11–13**, in which two ylide groups are introduced were found to have smaller E-C_C-E bond angles than the parent compounds with identical backbones. Comparison of the C_C-E bond lengths of **4–6** with those of **11–13** indicates that there is an increase in the C_C-E (both r_1 and r_2) bond lengths as a result of replacement of the amino groups with ylide centers. However, there is a decrease in the r_1 value and an increase in the r_2 value upon replacement of the two

methyl groups in **8–10** with the ylide centers in **11–13**. In the case of the six-membered NHCs with a saturated backbone (**14–16**), C_C–E (both r₁ and r₂) bond lengths are found to increase upon replacement of the amino groups with ylide centers. Similar results are also obtained for boron-substituted five- (**17–19**) and six- (**20–22**) membered NHCs. However, in all three cases, the change in the central E–C_C–E bond angle is not significant.

[3.1.3.2] Singlet–Triplet Separation and Thermodynamic Stabilities

As a first approximation, the stability of these molecules can be judged from their respective singlet–triplet energy gaps (ΔE_{S-T}) [12]. In general, the stability of the singlet state increases with an increase in the value of ΔE_{S-T} . The calculated ΔE_{S-T} values are given in Table 3.1.4.

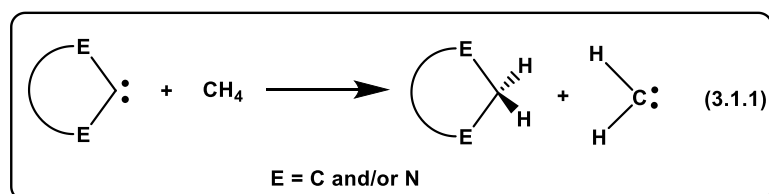
Table 3.1.4: PBE0/6-31+G* calculated singlet–triplet separations (ΔE_{S-T} , in kcal mol⁻¹) and stabilization energies (SE, in kcal mol⁻¹) of **1–22**.

Molecule	ΔE_{S-T}	SE	Molecule	ΔE_{S-T}	SE
1	43.9	79.4	12	59.9	114.3
2	40.3	72.6	13	64.2	115.8
3	39.6	69.8	14	58.0	101.9
4	55.3	103.6	15	50.3	97.7
5	59.4	114.5	16	50.4	107.3
6	63.5	114.6	17	43.6	82.3
7	61.7	113.9	18	35.3	86.9
8	40.4	84.7	19	31.7	90.4
9	37.1	77.3	20	42.2	87.7
10	36.8	74.9	21	39.6	86.4
11	57.5	105.8	22	40.6	95.8

It is evident from Table 3.1.4 that all of the molecules have a stable singlet ground state. The singlet state of **1** with a saturated backbone is slightly more stable than **2** with an unsaturated backbone. We did not observe any dramatic change in the stability of the singlet states as a result of the introduction of a nitrogen atom into the olefinic backbone. For example, the ΔE_{S-T} values of **2** and **3** (40.3 and 39.6 kcal mol⁻¹, respectively) and those of **9** and **10** (37.1 and 36.8 kcal mol⁻¹, respectively) are comparable. There is a significant increase in the ΔE_{S-T} values as a result of introduction

of the more-electron donating ylide groups (in **4–7**) in place of the two methyl groups (in **1–3**). On the other hand, replacement of the amino groups (in **1–3**) by ylidic ones (in **8–10**) decreases the ΔE_{S-T} values, albeit marginally. A comparison of the ΔE_{S-T} values of **8–10** with those of **11–13** shows that the introduction of one more ylide group dramatically enhances the stability. However, a comparison of **4–6** with **11–13** indicates that there is no significant increase in the ΔE_{S-T} values as a result of the replacement of the amine group with one more ylide group. Among the saturated six-membered NHCs (**14–16**), the parent carbene is found to have a higher ΔE_{S-T} value than those compounds with phosphorus ylide groups at α position with respect to the carbene carbon atom. Similarly, lower singlet–triplet separation is obtained for both five- and six-membered boron-substituted NHCs with ylide groups at α position to the C_C atom relative to the parent compounds. The changes are more appreciable for the five-membered ones.

The stabilization energies (SE) of **1–22** were evaluated by using equation (3.1.1) and these values were further used to obtain a measure of the thermodynamic stabilities of all of the molecules. It may be noted that the calculated stabilization energies are the same as indirect hydrogenation energies. The calculated values of the stabilization energies are listed in Table 3.1.4.



The stabilization energies of carbenes **1–13** follow an almost similar trend to the ΔE_{S-T} values. However, for molecules **14–22**, the stabilization energies do not go in parallel with the ΔE_{S-T} values. For example, the ΔE_{S-T} values of **17–19** are found to decrease as a result of the introduction of ylide groups, whereas the stabilization energies follow a reverse order. We obtained a reasonable correlation ($R^2=0.82$, with omission of the point corresponding to **19**, Figure 3.1.2) between the ΔE_{S-T} and SE values and both of these values predict **13** to be the thermodynamically most stable molecule. The singlet–triplet separation and stabilization energies of **4–6** and **11–13** are found to be comparable with the theoretically modeled experimentally known carbenes **1** and **7**. Similar comparisons can be made between the six-membered carbenes **15–16** and the boron-substituted carbenes **18–19** and **21–22** with the experimentally known carbenes **14**, **17** and **20**, respectively.

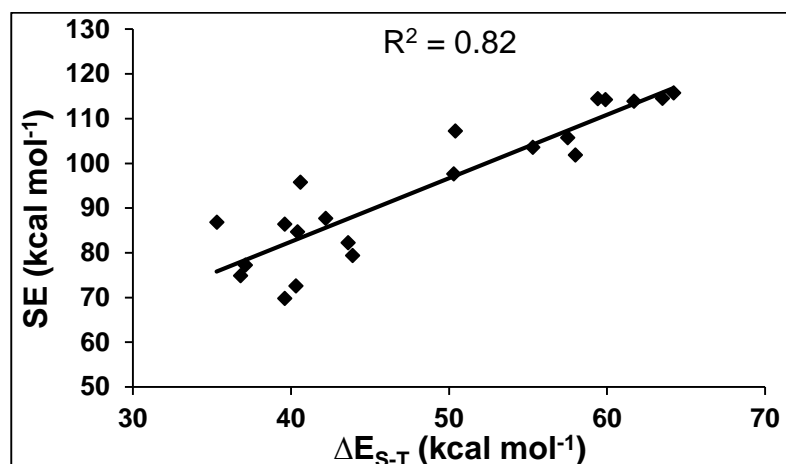


Figure 3.1.2: Correlation plot between calculated singlet-triplet separations (ΔE_{S-T}) and stabilization energies (SE) of 1-22.

[3.1.3.3] Ligand Properties

Both theoretical and experimental studies suggested that carbenes are very good σ donors [14, 15]. The σ -donating ability of carbene depends on the nature and energy of the σ -symmetric lone-pair orbital (E_{σ}) concentrated at the C_C atom [35]. The higher the energy of this frontier orbital, the higher the donating ability will be. We have performed NBO [33] analysis in order to determine the energies of these σ -donating frontier orbitals. The calculated E_{σ} values are listed in Table 3.1.5 and are graphically represented in Figure 3.1.3.

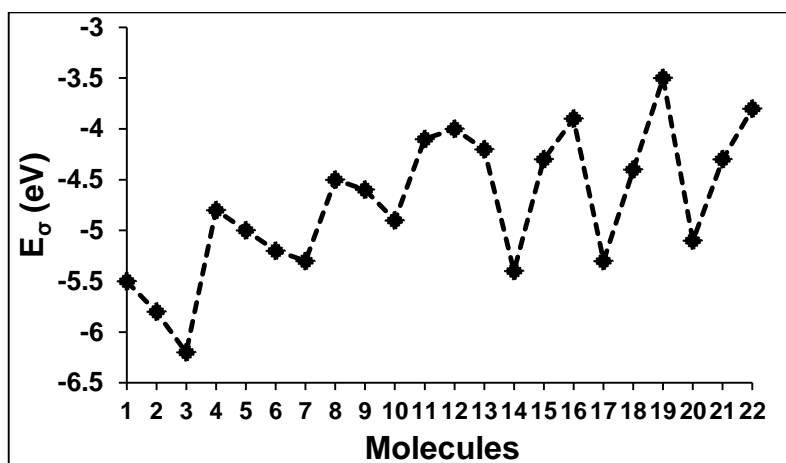


Figure 3.1.3: Plot of the energies of the σ -symmetric lone-pair orbitals (E_{σ} , in eV) concentrated at the central carbon atom of 1-22.

Table 3.1.5: PBE0/6-31+G* calculated energies (E_σ , in eV) and hybridization (% s-character) of the σ -symmetric lone-pair orbital concentrated at the carbene carbon atom and the respective proton affinity (PA, kcal mol⁻¹) values of **1–22**.

Molecule	E_σ	Hybridization (% s-character)	PA
1	-5.5	sp ^{1.20} (45.4)	270.5
2	-5.8	sp ^{1.09} (47.7)	266.0
3	-6.2	sp ^{1.09} (47.8)	256.6
4	-4.8	sp ^{1.48} (40.3)	291.8
5	-5.0	sp ^{1.29} (43.7)	292.9
6	-5.2	sp ^{1.26} (44.3)	287.4
7	-5.3	sp ^{1.30} (43.5)	284.0
8	-4.5	sp ^{1.70} (36.8)	295.0
9	-4.6	sp ^{1.44} (41.0)	294.5
10	-4.9	sp ^{1.44} (41.0)	285.9
11	-4.1	sp ^{1.98} (33.5)	308.3
12	-4.0	sp ^{1.68} (37.3)	313.1
13	-4.2	sp ^{1.65} (37.7)	308.4
14	-5.4	sp ^{1.23} (44.8)	267.5
15	-4.3	sp ^{1.79} (35.8)	293.2
16	-3.9	sp ^{2.60} (27.7)	309.4
17	-5.3	sp ^{1.03} (49.1)	275.2
18	-4.4	sp ^{1.49} (40.1)	297.9
19	-3.5	sp ^{1.81} (35.6)	311.2
20	-5.1	sp ^{1.11} (47.3)	274.9
21	-4.3	sp ^{1.63} (37.9)	294.7
22	-3.8	sp ^{2.25} (30.8)	307.8

Both Table 3.1.5 and Figure 3.1.3 indicate that there is a marginal decrease (except for **12**) in the σ -donating ability of carbenes **1–13** as a result of changes in the backbone. It is apparent from Figure 3.1.3 that replacement of the two methyl groups attached to the α -carbon atom with respect to the C_C atom in **1–3** by the more-electron-releasing ylide groups (in **4–7**) dramatically lifts the E_σ values and thereby significantly enhances the basicity of **4–7**. Similarly, replacement of the amino groups of **1–3** with ylide groups (in **8–10**) significantly increases the σ -donating abilities. The introduction

of two ylide centers near to the C_C atom (in **11–13**) is found to further increase the σ -donating ability. A similar increase in electron-donating ability is obtained for six-membered NHCs with a saturated backbone (**14–16**) and for both five- (**17–19**) and six- (**20–22**) membered boron-substituted NHCs. Out of all of the molecules, **19** is found to have the highest σ -donating ability.

In order to get a better understanding of the σ -donating ability of the carbenes considered for this study, we have analyzed the hybridization of the σ -symmetric lone-pair orbital (LP $_{\sigma}$) at the C_C atom, along with the percentage of s-character (Table 3.1.5). The E $_{\sigma}$ values increase with a decrease in the s-character of the lone pair at the C_C atom. Thus, molecules with lower s-character in the LP $_{\sigma}$ are found to have better σ -donating abilities. In fact, we obtained a good correlation ($R^2 = 0.79$) between the energies and the percentage of s-character of the σ -symmetric lone-pair orbitals at the C_C atom (Figure 3.1.4). The basicity of these carbene molecules can also be gauged from an evaluation of their respective proton affinities [36]. The higher the basicity, the higher the proton affinity (PA) will be. Accordingly, we have calculated the proton affinity values for all the carbenes molecules which are listed in Table 3.1.5. Interestingly, we obtained a nice correlation ($R^2 = 0.90$) between the computed E $_{\sigma}$ and PA values (Figure 3.1.5). In agreement with their enhanced σ -donating abilities, the PA values of the bis-ylide-containing carbenes are found to be significantly higher (>300 kcal mol⁻¹) than others.

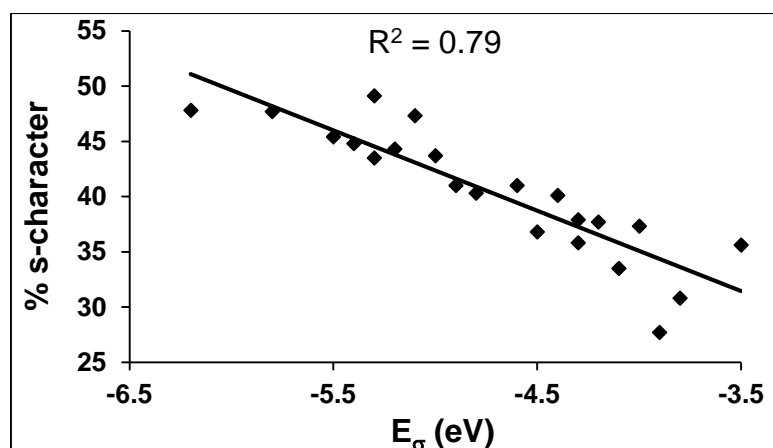


Figure 3.1.4: Correlation plot between the energies of the σ -symmetric lone-pair orbitals concentrated at the carbene center (E $_{\sigma}$, in eV) and percentage of s-character of the lone pair of **1–22**.

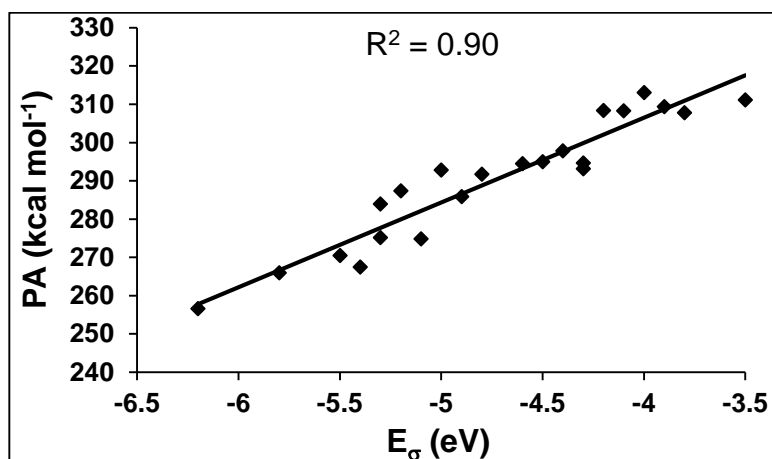
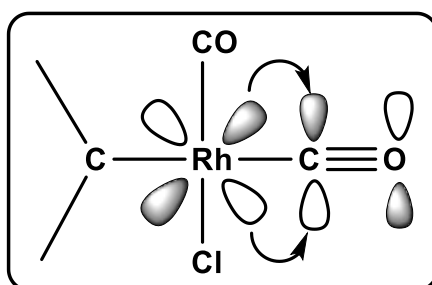


Figure 3.1.5: Correlation plot between the energies of the σ -symmetric lone-pair orbitals (E_{σ} , in eV) and proton affinity (PA, kcal mol⁻¹) values of **1–22**.

The carbonyl-stretching frequencies (ν_{CO}) of the corresponding metal carbonyl complexes can be used as an important tool to measure the σ -donating abilities of the carbene ligands [37]. The higher the σ basicity of a carbene ligand, the higher the electron density at the metal center will be and, consequently, the higher the extent of back donation from the metal center to the CO anti-bonding orbital will be (Scheme 3.1.2), which will thereby shift the carbonyl-stretching frequencies (ν_{CO}) to lower values.



Scheme 3.1.2: Schematic representation of the back-bonding interaction between the metal center and the CO antibonding (π^*) orbital.

To get a quantitative measure of the electron-donating ability of the carbene ligands under consideration, we have optimized square-planar complexes of rhodium, $L\text{-Rh}(\text{CO})_2\text{Cl}$ (L : **1–22**) with the two carbonyl groups in the *cis* positions. The calculated values of average carbonyl stretching frequencies ($\nu_{\text{CO}(\text{avg})}$) for all of the complexes are given in Table 3.1.6. The calculated $\nu_{\text{CO}(\text{avg})}$ values are found to vary as a function of the relative σ basicity of the carbene ligands. The computed $\nu_{\text{CO}(\text{avg})}$ values of the metal complexes containing ylide substituted carbenes are found to be appreciably lower than

Table 3.1.6: PBE0/6-31+G* calculated energies of the σ -symmetric lone-pair orbital concentrated at the carbene carbon atom (E_σ , in eV) and the average carbonyl stretching frequencies ($\nu_{\text{CO(avg)}}$, in cm^{-1}) of L–Rh(CO)₂Cl (L: **1–22**) complexes.

Molecule	E_σ	$\nu_{\text{CO(avg)}}$	Molecule	E_σ	$\nu_{\text{CO(avg)}}$
1	–5.5	2131	12	–4.0	2112
2	–5.8	2136	13	–4.2	2112
3	–6.2	2141	14	–5.4	2136
4	–4.8	2120	15	–4.3	2122
5	–5.0	2125	16	–3.9	2110
6	–5.2	2129	17	–5.3	2136
7	–5.3	2131	18	–4.4	2122
8	–4.5	2122	19	–3.5	2110
9	–4.6	2123	20	–5.1	2131
10	–4.9	2129	21	–4.3	2120
11	–4.1	2112	22	–3.8	2101

those of others. This indicates significantly enhanced electron donating abilities of the ylide-containing carbenes. Among all of the molecules, **3** is found to have the lowest σ -donating ability and, consequently, the $\nu_{\text{CO(avg)}}$ value of the respective rhodium complex is found to be the highest. Similarly, for molecules like **16**, **19** and **22**, which are better σ donors, the carbonyl-stretching frequencies are significantly lower than those of others. We have obtained a nice correlation ($R^2 = 0.88$) between the E_σ and $\nu_{\text{CO(avg)}}$ values (Figure 3.1.6).

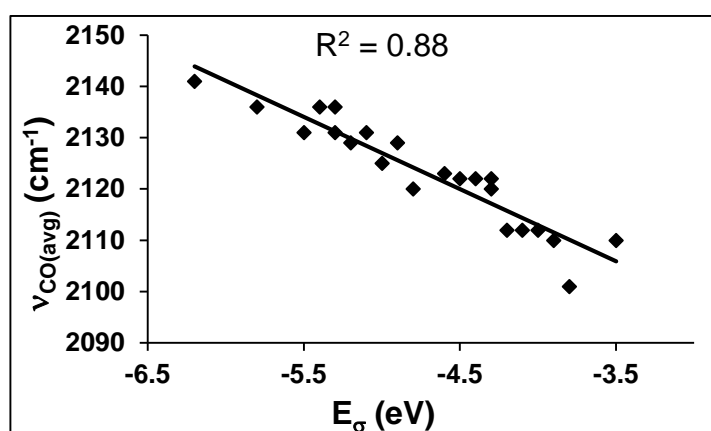


Figure 3.1.6: Correlation plot between the energies of the σ -symmetric lone pair orbitals concentrated at the central carbene carbon atom (E_σ , in eV) and the $\nu_{\text{CO(avg)}}$ values (in cm^{-1}) of the L–Rh(CO)₂Cl complexes (L: **1–22**).

[3.1.3.4] Nucleophilicity index

The donor strength of all of the carbene molecules was further assessed by evaluating their nucleophilicity indices. The nucleophilicity index (N) is calculated by using the equation $N = E_{HOMO} - E_{HOMO}(TCNE)$, with tetracyanoethylene (TCNE) considered as the reference [38]. The calculated values of the nucleophilicity indices are listed in Table 3.1.7.

Table 3.1.7: PBE0/6-31+G* calculated nucleophilicity indices (N , in eV), bond dissociation energies of the Ga-C_C bond (BDE, kcal mol⁻¹), degree of pyramidalization at the Ga atom (θ_{Ga} , in degree) and Ga-C_C bond lengths (r_{Ga-C_C} , in Å) of the GaCl₃ adducts of **1–22**.

Molecule	N	BDE	θ_{Ga}	r_{Ga-C_C}
1	4.1	62.6	31.1	2.024
2	3.7	64.8	28.5	2.017
3	3.4	61.3	26.1	2.022
4	4.8	77.2	38.1	1.995
5	4.6	83.4	37.5	1.976
6	4.4	82.2	34.5	1.974
7	4.3	80.2	35	1.981
8	5.1	78.8	38.8	1.998
9	5.0	83.6	35.4	1.979
10	4.7	80.7	32.8	1.982
11	5.9	83.7	44.1	1.987
12	5.6	95.8	44.5	1.957
13	5.4	95.4	41.4	1.957
14	4.2	58.4	28.1	2.049
15	5.3	71.4	36.2	2.017
16	5.9	75.4	45.3	2.001
17	4.3	60.7	27.7	2.036
18	5.2	75.0	35.6	2.012
19	6.1	80.3	44.7	1.997
20	4.5	62.5	30.3	2.049
21	5.3	72.3	37.6	2.019
22	5.8	75.5	44.4	2.011

The nucleophilicity indices of the carbene molecules are found to be in the range of 3.4–6.1 eV. These values show a similar trend to the respective E_σ values. The values of the nucleophilicity indices support the increase in σ -donating ability of carbenes as a result of the introduction of ylide centers into the ring framework. The N values are found to be highest for carbenes with two ylide groups adjacent to the C_C atom. The highest and lowest σ basicities are obtained for **19** and **3** (Table 3.1.5) respectively, which is in agreement with their respective N values. Indeed, we have obtained an excellent correlation ($R^2 = 0.98$) between the E_σ and N values (Figure 3.1.7).

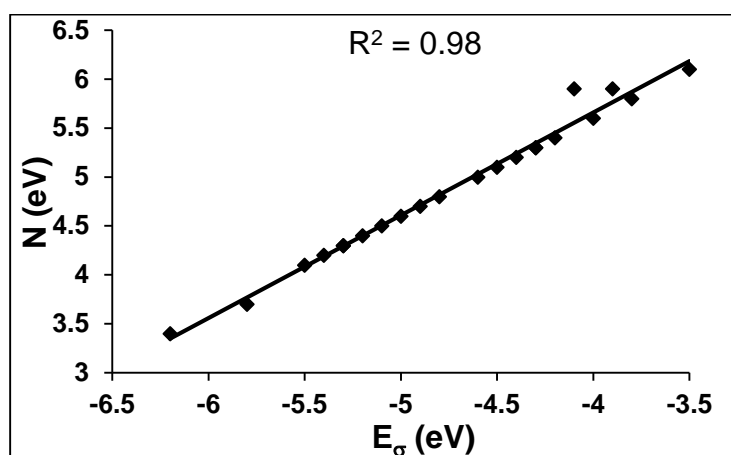
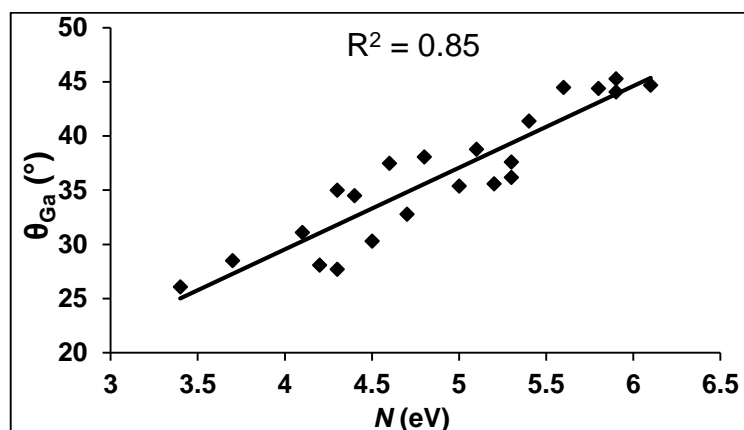
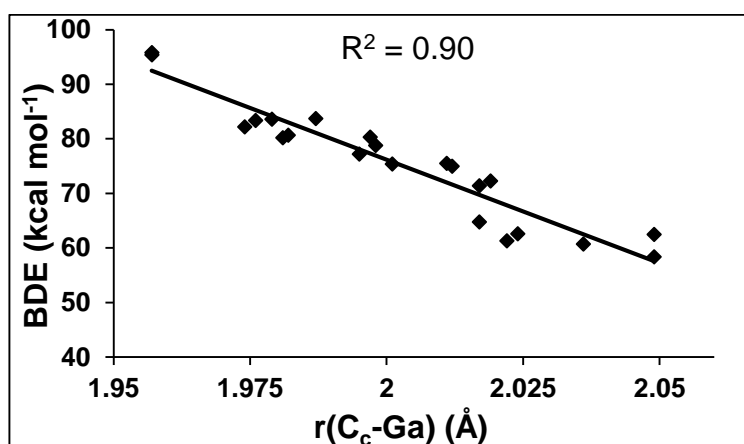


Figure 3.1.7: Correlation plot between energies of the σ -symmetric lone pair orbitals (E_σ , in eV) and nucleophilicity indices (N , in eV) for **1–22**.

Recently, Gandon and co-workers have shown that the nucleophilicity of a carbene ligand may be correlated with the degree of gallium pyramidalization (θ_{Ga} ; $\theta_{Ga}=360^\circ-\sum(\text{Cl-Ga-Cl})$) in the carbene adducts of GaCl_3 [39]. By following this approach, we have calculated the GaCl_3 adducts of **1–22** and the computed values are listed in Table 3.1.7. Interestingly, we obtained a good correlation ($R^2 = 0.85$) between N and θ_{Ga} values (Figure 3.1.8(a)) as well as a nice correlation ($R^2 = 0.90$) between the Ga-C_C bond dissociation energies and bond lengths (Figure 3.1.8(b)). Furthermore, we have also obtained a nice correlation ($R^2 = 0.92$) between the calculated proton affinity and the degree of Ga pyramidalization (Figure 3.1.9).



(a)



(b)

Figure 3.1.8: Correlation plots between (a) the pyramidalization angle at the gallium atom (θ_{Ga} , in degrees) and the nucleophilicity indices (N , in eV), and (b) the Ga-C_C bond dissociation energies (BDE, in kcal mol⁻¹) and the Ga-C_C bond lengths (in Å) of the GaCl₃ adducts of **1–22**.

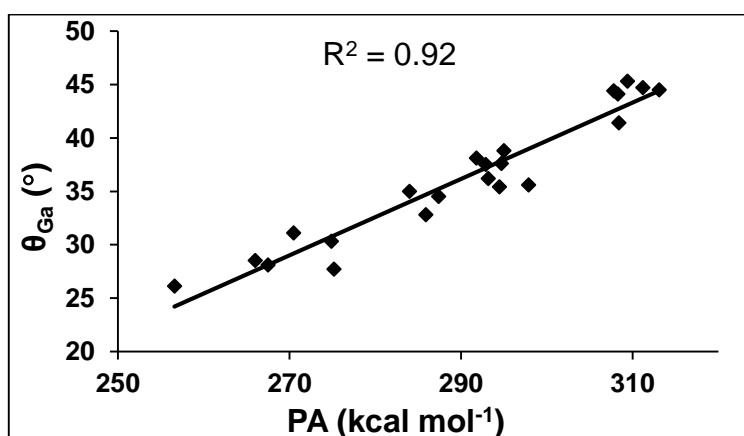


Figure 3.1.9: Correlation plot between the calculated proton affinities (kcal mol⁻¹) and pyramidalization angle at gallium atom (θ_{Ga}) of the GaCl₃ adducts of **1–22**.

[3.1.4] Conclusions

Density functional theory calculations have been carried out on a number of cyclic carbene molecules with or without heteroatoms in the ring framework. All of these molecules exhibit a stable singlet ground state. The introduction of ylide centers into the ring framework was found to dramatically enhance the σ -donating ability. Furthermore, for majority of the molecules, ylide substitution leads to a significant increase in stability. The carbonyl-stretching frequencies of the corresponding metal complexes and the nucleophilicity index values were found to correlate well with the σ basicity of these carbenes. The calculated proton affinity values and the extent of Ga pyramidalization were also in excellent agreement with the σ basicity of these carbenes. We hope that our study will trigger new experimental studies towards the exploration of novel ylide-stabilized carbenes.

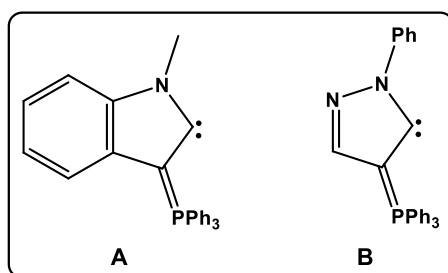
[3.2] Theoretical Strategies Toward Stabilization of Singlet Remote *N*-Heterocyclic Carbenes.

[3.2.1] Introduction

Following the discovery of the first stable singlet carbene by Bertrand et al. in 1988, Arduengo et al. synthesized the first bottleable singlet *N*-heterocyclic carbene (NHC), 1,3-di(1-adamantyl)imidazol-2-ylidene in 1991 [2,40]. Since then a number of derivatives of NHCs have been synthesized in their singlet state. The primary stabilizing factor of these NHCs is the π donation from the nitrogen lone pairs to the formally vacant p orbital of the carbene carbon (C_C). The greater the donation from the nitrogen lone pairs, the higher the stability of the singlet state of the NHCs will be. In 1,3-di(1-adamantyl)imidazol-2-ylidene, in addition to this electronic factor, the steric protection provided by the two adamantyl groups attached to the nitrogen atoms also contribute to their singlet-state stability. However, one year later, the isolation of 1,3,4,5-tetramethylimidazol-2-ylidene indicated that electronic factors alone may be sufficient to stabilize the singlet state of NHCs [9]. NHCs are found to have excellent σ -donation as well as considerable π -accepting abilities [14,15].

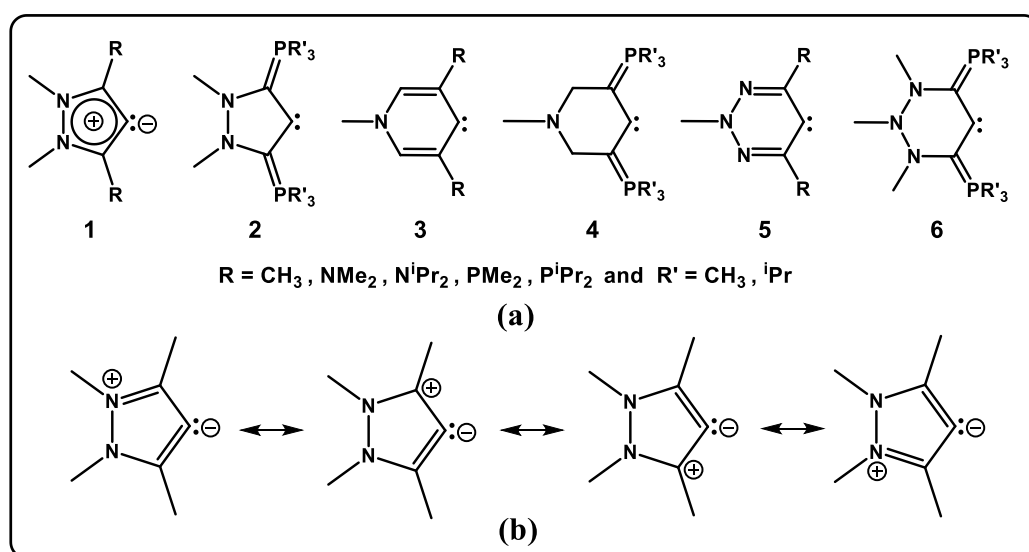
In addition to these NHCs, NHC variants known as remote NHCs (rNHCs) have drawn the attention of several researchers due to the excellent catalytic activity of their metal complexes [41]. The structural difference with their normal analogs is that here, the heteroatom(s) are away from the carbenic center. A number of transition metal complexes containing rNHCs as ligands were reported and found to have remarkable catalytic activities [42]. Theoretical calculations suggested that rNHCs are better σ -donors as well as better π -acceptors than their normal NHC counterparts [43]. Indeed, Pd(II)-rNHC complexes were found to be more effective catalysts in C-C coupling reactions compared to those using Pd(II)-NHC complexes [43a]. We are motivated by the fact that despite their better ligand properties, so far no rNHCs have been isolated in their free state [44], which may be traced to their low singlet-triplet energetic separations. Unlike in normal NHCs, π stabilization is not so effective in rNHCs resulting in lower singlet-triplet separations. In rNHCs, the nitrogen atoms are further from the carbene center and hence the electronic delocalization from the nitrogen lone pairs to the formally vacant p orbital of the carbene carbon (which is responsible for the singlet ground state stability) is not as effective as in NHCs. Consequently, the singlet-triplet separations of rNHCs are lower than those of their normal counterparts. We

envisage that any factor (for example installation of π -donor substituents like NMe_2 near to the carbene center) that can increase the singlet-triplet separations of rNHCs may help to stabilize or even allow them to be isolated in the singlet state as free carbenes. In a couple of seminal contributions, Kawashima (**A**, Scheme 3.2.1) [24a] and Fürstner (**B**, Scheme 3.2.1) [24b] showed that installation of phosphorus ylides near to the carbene carbon not only stabilizes the carbene in its singlet state but also significantly enhances their σ -donation ability. The stabilization of the singlet state comes from effective π -donation from the ylidic carbanion to the formally vacant p orbital at the carbene center.



Scheme 3.2.1: Schematic representation of experimentally known aminoylidecarbenes [24a–b].

Thus, it may be rewarding to consider phosphorus ylides as substituents towards stabilization of rNHCs as free singlet carbenes. Herein, we present the results of theoretical studies aimed toward stabilization of five- and six-membered remote carbenes in their ground singlet states (Scheme 3.2.2).



Scheme 3.2.2: (a) Range of molecules considered for this study and (b) The four possible resonance structures for rNHC **1**.

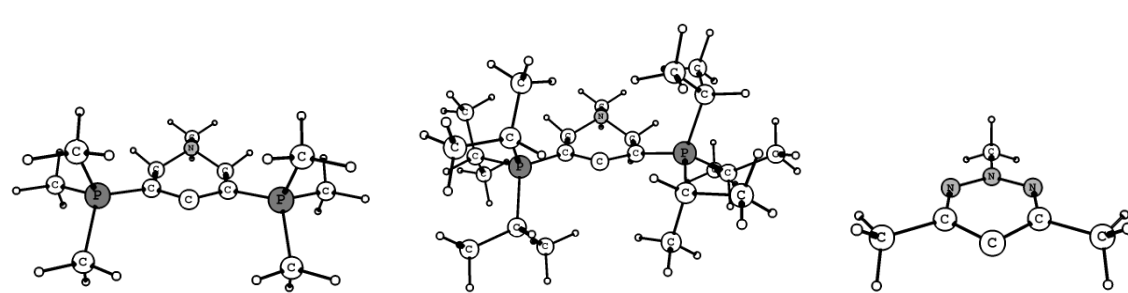
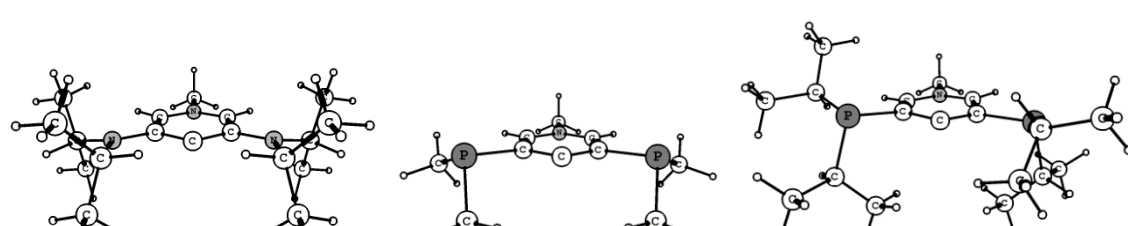
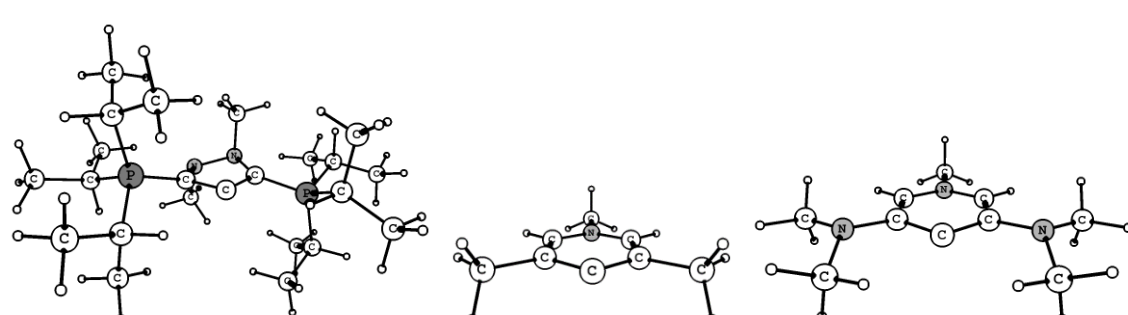
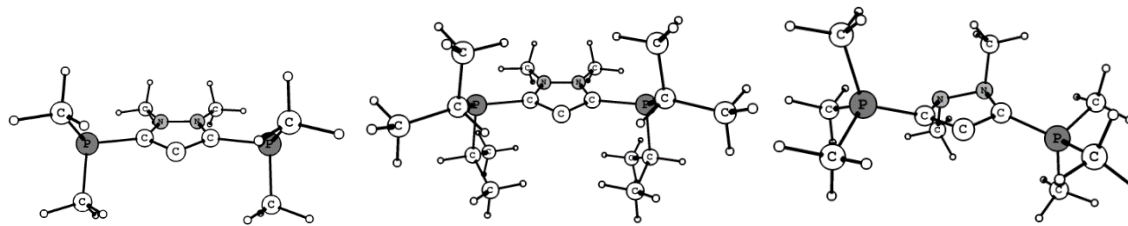
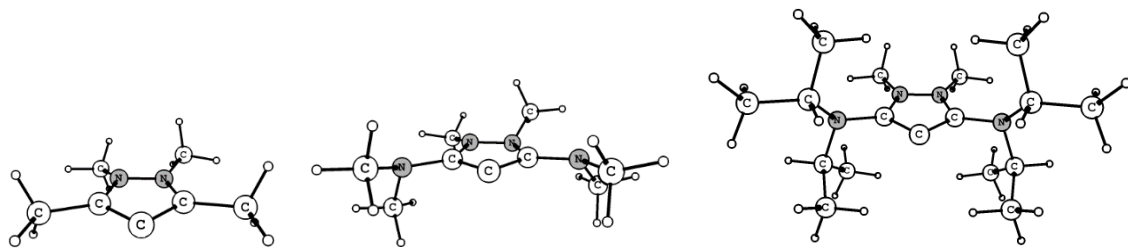
[3.2.2] Computational Details

Geometry optimization of all the molecules were carried out using PBE0 exchange-correlation functional [26] and 6-31+G* basis set for the main group elements while the SDD basis set with the Stuttgart–Dresden relativistic effective core potential for the rhodium atom [27]. This level of theory was found to be adequate in dealing with similar systems as reported recently [28,29]. To reduce the computational cost, we simplified the experimentally known phosphorus ylides by substituting the bulky phenyl (Ph) groups with methyl (Me) and isopropyl (ⁱPr) groups (see Scheme 3.2.2). Frequency calculations were performed at the same level of theory to characterize the nature of the stationary point. All structures were found to be minima on the potential energy surface with real frequencies. Natural bonding analyses were performed with the natural bond orbital (NBO) partitioning scheme [33] as implemented in the Gaussian 03 suite of programs [34]. The interatomic magnetizabilities were calculated by the Proaim basin integration approach as implemented in the AIMALL suite of programs [45]. The wfx files for the computation of magnetizabilities were generated through the fchk files using the AIMALL program. The fchk files were obtained from NMR calculations performed at the same level of theory.

[3.2.3] Results and Discussion

[3.2.3.1] Molecular Geometries

The optimized singlet state geometries of molecules **1**, **3** and **5** comprise a planar central carbene ring structure whereas for the molecules having ylide groups as substituents at the carbon atom α to the carbene center (**2**, **4** and **6**), optimization leads to non-planar structures (Figure 3.2.1). The calculated geometrical parameters for both singlet and triplet states are listed in Table 3.2.1. In both the singlet and triplet states, the central $C_{\alpha}-C_C-C_{\alpha'}$ bond angle of the five-membered rNHCs are found to be smaller than those of the six-membered ones. Except in **1PMe₂** and **2PMe₃**, for all other rNHCs, the central carbene bond angle is found to be larger in the triplet state than the stable singlet state. Barring few cases, all the rNHCs have similar C–C_C bond lengths for both sides of the carbene center. However, in some cases, despite having a symmetrical backbone, the C–C_C bond lengths are found to be different which may be reasoned to the different orientations of the substituents at C_α. For both the singlet and triplet states of **1**, the central $C_{\alpha}-C_C-C_{\alpha'}$ bond angle is almost constant for all the molecules indicating



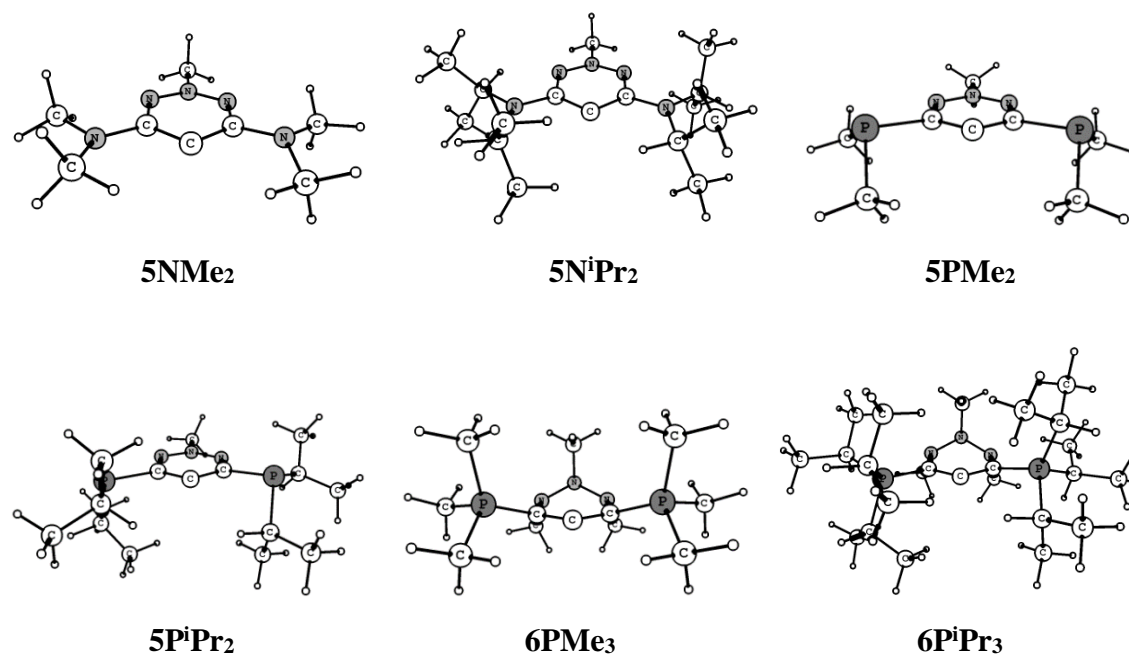


Figure 3.2.1: Optimized singlet-state geometries of all the remote carbenes (**1-6**).

negligible effect of substituents. In case of the six-membered ones, **5** and **6** have reduced $C_{\alpha}-C_{\beta}-C_{\beta'}$ bond angle in both singlet and triplet states than that in **3** and **4**. A comparison between the singlet state geometries of **3Me** and **4** indicates that ylide substitution slightly increases the central $C_{\alpha}-C_{\beta}-C_{\beta'}$ bond angle (by $1-2^{\circ}$) but decreases the $C-C_{\beta}$ bond lengths (by 0.02 \AA). However, similar comparison between **5Me** and **6** shows that the increase in $C_{\alpha}-C_{\beta}-C_{\beta'}$ bond angle is more pronounced (by 4°) while the decrease in $C-C_{\beta}$ bond lengths is almost same (by 0.02 \AA). In case of **3NMe₂** and **3NiPr₂**, the $C-C_{\beta}$ bond lengths for both the singlet and triplet states are found to be same although they have wider $C_{\alpha}-C_{\beta}-C_{\beta'}$ bond angle in the triplet states than the corresponding singlet states.

Table 3.2.1: PBE0/6-31+G* calculated values of C_C-C_α bond lengths (in Å) and C_α-C_C-C_{α'} bond angles (in degree) for both singlet and triplet states of **1-6**.

Molecule	R/R'	r(C _C -C _α)		∠C _α -C _C -C _{α'}	
		Singlet	Triplet	Singlet	Triplet
1	CH ₃	1.399/1.399	1.372/1.372	101.2	113.1
	NMe ₂	1.398/1.388	1.405/1.362	99.9	111.2
	N ⁱ Pr ₂	1.396/1.396	1.376/1.376	101.0	112.8
	PMe ₂	1.399/1.399	1.405/1.433	101.5	101.5
	P ⁱ Pr ₂	1.404/1.404	1.375/1.374	101.7	113.9
2	PMe ₃	1.407/1.407	1.398/1.398	100.7	100.5
	P ⁱ Pr ₃	1.408/1.408	1.384/1.412	101.8	102.9
3	CH ₃	1.423/1.423	1.404/1.404	113.6	124.1
	NMe ₂	1.408/1.408	1.405/1.405	115.7	124.6
	N ⁱ Pr ₂	1.408/1.408	1.406/1.406	117.7	126.4
	PMe ₂	1.423/1.423	1.404/1.404	113.7	124.6
	P ⁱ Pr ₂	1.427/1.422	1.420/1.387	113.9	124.6
4	PMe ₃	1.402/1.402	1.372/1.362	114.7	124.2
	P ⁱ Pr ₃	1.409/1.400	1.418/1.402	115.8	120.9
5	CH ₃	1.415/1.415	1.396/1.396	110.4	121.2
	NMe ₂	1.403/1.403	1.396/1.396	111.2	120.5
	N ⁱ Pr ₂	1.404/1.404	1.395/1.399	112.4	121.8
	PMe ₂	1.414/1.414	1.394/1.394	110.2	121.1
	P ⁱ Pr ₂	1.419/1.409	1.398/1.391	110.9	121.6
6	PMe ₃	1.398/1.398	1.379/1.370	114.2	115.9
	P ⁱ Pr ₃	1.403/1.396	1.404/1.359	114.9	130.1

[3.2.3.2] Singlet-Triplet Separation

The singlet-triplet separations (ΔE_{S-T}) of carbene molecules can be used as a measure of their stability [12]. In principle, the higher the values of ΔE_{S-T} , the higher the stability of the carbene molecule will be in its singlet state. The calculated values of ΔE_{S-T} for all the molecules are listed in Table 3.2.2. For the sake of comparison, the ΔE_{S-T} values of five and six-membered normal NHCs (**5NHC** and **6NHC**) calculated at the same level of theory [28a] are also included in Table 3.2.2.

Table 3.2.2: PBE0/6-31+G* calculated values of singlet-triplet separations (ΔE_{S-T} , in kcal mol⁻¹) and natural charges at C_C ($q(C_C)$) for molecules **1–6**.

Molecule	R/R'	ΔE_{S-T}	$q(C_C)$
1	CH ₃	37.5	-0.423
	NMe ₂	45.5	-0.478
	N ⁱ Pr ₂	45.9	-0.456
	PMe ₂	38.1	-0.400
	P ⁱ Pr ₂	36.6	-0.406
2	PMe ₃	47.8	-0.305
	P ⁱ Pr ₃	46.8	-0.301
3	CH ₃	19.6	-0.218
	NMe ₂	28.3	-0.304
	N ⁱ Pr ₂	28.5	-0.319
	PMe ₂	19.9	-0.204
	P ⁱ Pr ₂	15.7	-0.191
4	PMe ₃	51.3	-0.296
	P ⁱ Pr ₃	46.9	-0.281
5	CH ₃	13.2	-0.262
	NMe ₂	20.2	-0.374
	N ⁱ Pr ₂	20.9	-0.397
	PMe ₂	13.9	-0.263
	P ⁱ Pr ₂	13.2	-0.273
6	PMe ₃	61.2	-0.363
	P ⁱ Pr ₃	46.6	-0.329
5NHC		81.3	
6NHC		58.0	

It is evident from Table 3.2.2 that while the ΔE_{S-T} value for the normal five-membered NHC (**5NHC**) is 81.3 kcalmol⁻¹, it is only 37.5 kcalmol⁻¹ for the structurally similar remote counterpart. This can be attributed to reduced π -stabilization in **1Me** compared with **5NHC**. However, introduction of π -electron donating substituents (NMe₂ and NⁱPr₂) at C _{α} was found to increase the singlet-triplet separation of both five- (**1**) and six-membered (**3** and **5**) rNHCs (Table 3.2.2). This indicates an increase in the stability of the singlet ground state. However, there is no significant change in the ΔE_{S-T} values as a result of introduction of PMe₂ and PⁱPr₂ groups. This can be attributed to the inability

of phosphorus to share its lone pair with the formally vacant p_{π} orbital of C_C which in turn can be traced to the higher inversion barrier of phosphorus compared to nitrogen. In fact, NBO analysis shows a significant increase in natural charge at C_C for rNHCs having NMe_2 and N^iPr_2 substituents compared to those with PMe_2 and P^iPr_2 as substituents at C_{α} (Table 3.2.2). In addition, in the case of the six-membered rNHCs, the C_C-C_{α} bond lengths for rNHCs with NMe_2 and N^iPr_2 as substituents are shorter than the parent rNHCs with methyl substituents while no appreciable changes are obtained for PMe_2 - and P^iPr_2 -substituted derivatives (Table 3.2.1). NBO-based second order perturbation analysis indicated a stabilizing interaction resulting from delocalization of the nitrogen lone pair (N_{LP}) from NMe_2 or N^iPr_2 to the $C_{\alpha}-C_{\beta}$ (with respect to C_C) antibonding orbital, which results in an elongation of the $C_{\alpha}-C_{\beta}$ bonds in **3** and **5** (for $R = NMe_2/N^iPr_2$). We observed a dramatic increase in singlet-triplet gap as a result of installation of electron-donating ylidic groups at C_{α} (**2**, **4** and **6**) with the effect being more prominent for the six-membered rNHCs than the five-membered ones (Table 3.2.2). Among all the rNHCs, **6PMe3** is found to have the highest stability ($\Delta E_{S-T} = 61.2$ kcal mol⁻¹). Interestingly, this ΔE_{S-T} value is also higher than that of the six-membered normal NHC with a saturated backbone (**6NHC**, Table 3.2.2). Such a stabilization of the singlet state results from effective π -donation of the ylidic carbanion to the carbene center [24]. Accordingly, we observed shorter C_C-C_{α} bond lengths for the ylide-stabilized carbenes than those for others (Table 3.2.1). Interestingly, the calculated singlet-triplet gap of ylide stabilized rNHCs falls within the range (45.0–85.0 kcal mol⁻¹) of known carbenes [46], and to the best of our knowledge, no rNHCs are currently known with such large computed singlet-triplet gaps. Thus, rNHCs **2**, **4** and **6** could be promising candidates for possible experimental realization as free remote carbenes. In order to check the reliability of the computed singlet-triplet gaps, we have re-optimized **6PMe3** at different levels of theory using a larger basis set as a representative case [47] and obtained comparable values (Table 3.2.3). The singlet-triplet gap of **6PMe3** increases to 69.1 kcal mol⁻¹ at the M06-2X/6-311++G* level of theory and further increases to 72.4 kcal mol⁻¹ on being computed using the dispersion corrected wB97XD functional. NBO analysis indicates delocalization of electronic charge from the carbanion of the ylidic system to the $C_C-C_{\alpha}/C_C-C_{\alpha}$ antibonding orbital. An MO analysis of **6PMe3** shows that despite its non-planarity (the N atom trans to C_C is projected out of the plane formed by the other five ring atoms, Figure 3.2.1), there exists a ring current generated by cyclic

Table 3.2.3: Calculated values of singlet-triplet gaps (ΔE_{S-T} , in kcal mol⁻¹) of **6PMe₃** using different basis sets and functionals.

Level of Theory	ΔE_{S-T}
PBE0/6-31+G*	61.2
B3LYP/6-311++G*	57.8
M06/6-311++G*	52.7
M06-2X/6-311++G*	69.1
wB97XD/6-311++G*	72.4

delocalization of electrons involving the lone pairs on the two β -nitrogen atoms (with respect to C_C), occupied p_π orbitals of the ylidic carbanions and the formally vacant p -orbital of the carbenic carbon atom (Figure 3.2.2(a)). The delocalized bonding pattern present in **6PMe₃** can also be visualized by plotting the laplacian of the calculated electronic charge density in the plane of the ring (Figure 3.2.2(b)) where the areas of local charge concentration are distributed over the atomic basins of the five in-plane (3C and 2N) ring atoms. Similar electronic delocalization is also observed in **6PⁱPr₃** (Figure 3.2.3) although it has a comparatively lower ΔE_{S-T} value (46.6 kcal mol⁻¹) than **6PMe₃**. This significant difference in the ΔE_{S-T} values can be attributed to the greater extent of

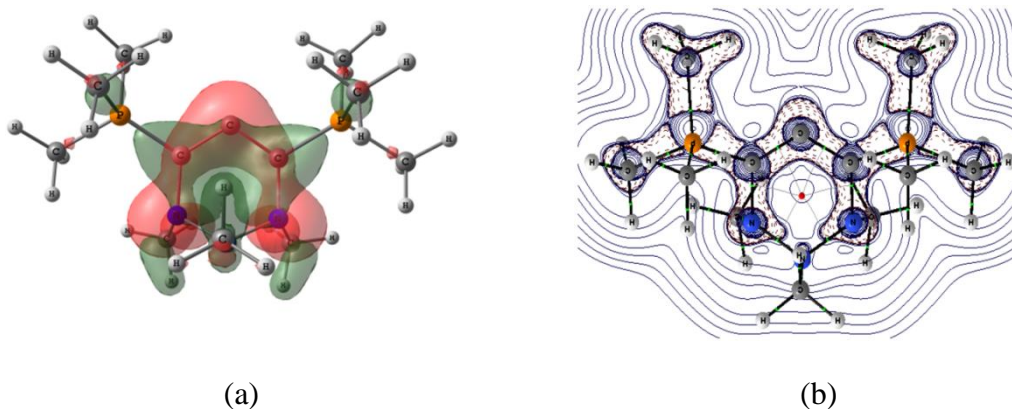


Figure 3.2.2: (a) Contour plots of molecular orbitals showing cyclic delocalization of electrons within the five atom ring of **6PMe₃** and (b) Contour line diagram of the Laplacian of electron density in the ring plane of **6PMe₃**. Solid blue lines indicate regions of charge depletion [$\nabla^2\rho(r)>0$] and dashed maroon lines indicate regions of charge concentration [$\nabla^2\rho(r)<0$]. Green and red spheres denote bond critical points (bcp) and ring critical points (rcp), respectively.

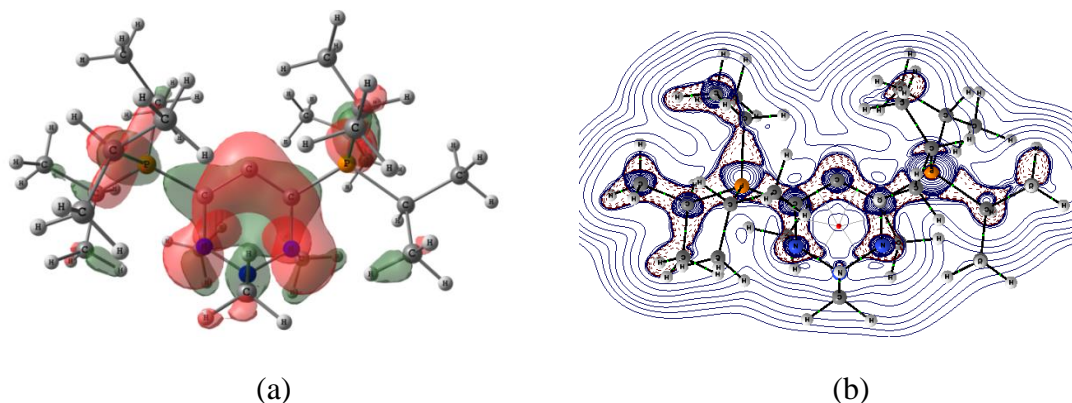


Figure 3.2.3: (a) Contour plots of molecular orbitals showing cyclic delocalization of electrons within the five atom ring of **6PⁱPr₃** and (b) Contour line diagram of the Laplacian of electron density in the ring plane of **6PⁱPr₃**. Solid blue lines indicate regions of charge depletion [$\nabla^2\rho(r)>0$] and dashed maroon lines indicate regions of charge concentration [$\nabla^2\rho(r)<0$]. Green and red spheres denote bond critical points (bcp) and ring critical points (rcp), respectively.

stabilization of the triplet state in **6PⁱPr₃** compared with that in **6PMe₃**. While the central $C_\alpha-C-C_\alpha$ bond angle differs marginally between the singlet and triplet state in **6PMe₃**, the same increases dramatically in the triplet state for **6PⁱPr₃** (Table 3.2.1). Also, the C_C-C_α bond is shorter in the triplet state of **6PⁱPr₃** than that in **6PMe₃**. This indicates that the triplet state is stabilized to a greater extent in **6PⁱPr₃** compared with that in **6PMe₃**, which results in lowering of the singlet-triplet gap.

[3.2.3.3] Aromaticity–NICS and QTAIM Analysis

To judge the extent of ring current present in all the molecules, we performed Nucleus Independent Chemical Shift (NICS) [48] calculations by placing a ghost atom (Bq) at the geometric centre as well as 1 Å above the plane of the central ring, leading to values denoted as NICS(0) and NICS(1) respectively. NICS is defined as the negative of the absolute magnetic shielding computed at the geometrical center point of the ring. Aromatic rings are characterized by negative NICS values (diatropic) and antiaromatic compounds by positive NICS values (paratropic). The calculated NICS values for all the molecules are given in Table 3.2.4.

The calculated NICS values of **1**, **3** and **5** with six π electrons are very close to those of benzene [NICS(0) = -8.2 and NICS(1) = -10.2] thereby supporting the aromatic nature of these molecules. Even though carbenes **2** are formally antiaromatic with 8π

Table 3.2.4: PBE0/6-31+G* calculated NICS(0) and NICS(1) values of molecules **1–6**.

Molecule	R/R'	NICS(0)	NICS(1)
1	CH ₃	-11.0	-9.9
	NMe ₂	-9.7	-8.2
	N ⁱ Pr ₂	-12.3	-10.1
	PMe ₂	-11.9	-11.4
	P ⁱ Pr ₂	-11.6	-11.1
2	PMe ₃	-5.1	-4.2
	P ⁱ Pr ₃	-5.3	-3.9
3	CH ₃	-7.2	-10.4
	NMe ₂	-7.9	-9.1
	N ⁱ Pr ₂	-6.5	-8.0
	PMe ₂	-5.3	-8.1
	P ⁱ Pr ₂	-5.5	-9.8
4	PMe ₃	-1.3	-2.6
	P ⁱ Pr ₃	-1.6	-3.3
5	CH ₃	-5.8	-11.2
	NMe ₂	-4.4	-8.2
	N ⁱ Pr ₂	-3.5	-7.3
	PMe ₂	-3.2	-9.2
	P ⁱ Pr ₂	-3.3	-9.6
6	PMe ₃	-2.4	-6.4
	P ⁱ Pr ₃	-2.2	-5.1

electrons, their computed NICS values are significantly negative indicating the presence of a considerable amount of ring current within the five-membered ring. Such a decrease in antiaromaticity can be explained by the involvement of the formally vacant carbene p_π orbital in cyclic delocalization within the ring. Indeed, we obtained an MO showing delocalization of electrons in **2** (Figure 3.2.4) involving the carbene p_π orbital, two ylidic carbanions and the lone pairs on two nitrogen atoms (through its backside lobe). However, even though carbenes **4** are formally six π electron systems (4π and 2π electrons from the two ylidic carbanions and N_{LP} respectively), they possess significantly less negative NICS values (compared with other 6π systems, i.e., **1**, **3** and **5**) implying their homoaromatic [49] nature. This is because not all the π electrons can participate in cyclic delocalization because of the presence of two saturated CH_2 groups within the

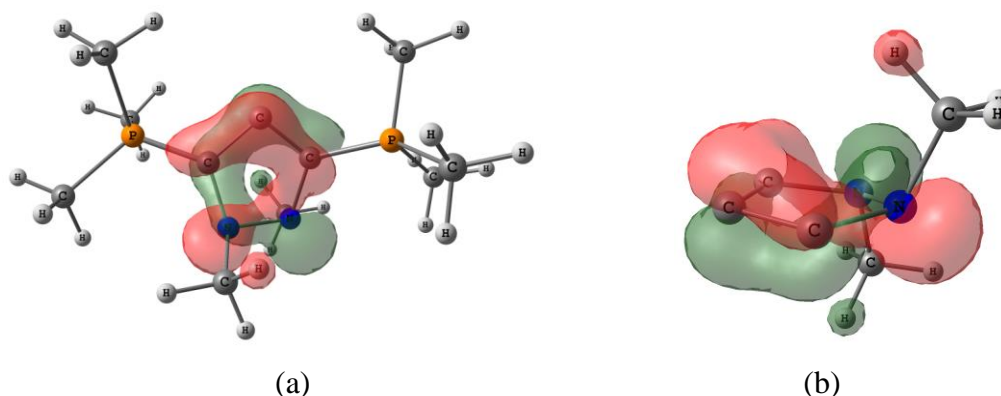


Figure 3.2.4: Contour plots showing cyclic delocalization of electrons involving all the five ring atoms of **2PMe₃**, (a) top view and (b) side view (PMe₃ groups are omitted for clarity).

ring. Moreover, the nitrogen lone pair is unable to take part in conjugation as the nitrogen atom is projected out of the plane of the ring. Similar is the case with carbenes **6**, which despite formally possessing **10** π electrons, are slightly less aromatic than **1**, **3** and **5**. Such reduced aromaticity of **6** may be traced to the inability of all the π electrons to take part in cyclic delocalization because of the nonplanar nature of the ring (the nitrogen atom γ to the carbene carbon is projected out of the plane, Figure 3.2.1). The remaining five atoms having eight π electrons should exhibit antiaromaticity. However, as in all other cases, the involvement of the formally vacant p orbital at C_C facilitates delocalization within the ring thereby making it moderately aromatic (their NICS(1) values are more than half of that for benzene).

QTAIM-based evaluation of inter-atomic magnetizability or bond magnetizability can be used as a direct measure of the current flux between two adjacent atomic basins and hence to predict the extent of aromatic delocalization within a ring system [50]. Accordingly, we have calculated isotropic as well as out-of-plane interatomic magnetizability values for some representative molecules (Table 3.2.5). For a comparison purpose, these values were also evaluated for benzene (an ideal aromatic system) at the same level of theory. Both the isotropic and out-of-plane bond magnetizabilities are found to be highly negative for benzene compared with others which is in accordance with its aromatic nature. Interestingly, the computed interatomic magnetizabilities (notably the out-of-plane magnetizabilities) for rNHCs **1Me**, **3Me** and **5Me** are found to be significantly negative and close to that of benzene. Thus, it can be concluded that the aromatic delocalization present in these rNHCs is evidenced from both the calculated NICS and bond magnetizability values.

Table 3.2.5: Average isotropic [$\chi(\text{C}/\Omega)$] and out-of-plane [$\chi_{zz}(\text{C}/\Omega)$] interatomic magnetizability values in cgs-ppm units (where $\Omega = \text{C}/\text{N}$).^a

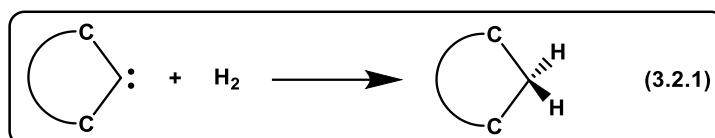
Molecule	$\chi(\text{C}/\Omega)$	$\chi_{zz}(\text{C}/\Omega)$
Benzene	-2.22	-4.93
1Me	-1.68	-3.64
2PMe₃	-1.41	-1.12
3Me	-1.74	-4.25
4PMe₃	-1.03	-1.65
5Me	-1.56	-3.87
6PMe₃	-1.20	-1.72

^aThe out-of-plane N atoms (in **4PMe₃** and **6PMe₃**) were not considered when evaluating these magnetizability parameters.

However, for the other representative systems (i.e., **2PMe₃**, **4PMe₃** and **6PMe₃**) bond magnetizabilities are found to be less negative, indicating less cyclic electronic delocalization within the ring.

[3.2.3.4] Hydrogenation and Dimerization Energies

The thermodynamic stabilities of all the molecules were further assessed by evaluating their hydrogenation energies (E_{hydro}) using equation (3.2.1). The calculated hydrogenation energies are listed in Table 3.2.6 and graphically represented in Figure 3.2.4. For the sake of comparison, the E_{hydro} values of five and six-membered normal NHCs (**5NHC** and **6NHC**) calculated at the same level of theory [28a] are also included in Table 3.2.6.



The less negative the values of hydrogenation energies, the higher the stability of the parent system will be. It is clear from both Table 3.2.6 and Figure 3.2.5 that the hydrogenation energies of molecules **1**, **3** and **5** show similar trends like the singlet-triplet separations. Installation of NMe_2 and N^iPr_2 at C_α significantly increases the hydrogenation energies, whereas PMe_2 and P^iPr_2 have negligible effects in increasing the hydrogenation energy for reasons explained earlier. Further, in the case of five-membered rNHCs, the hydrogenation energies are more negative for those having ylide substituents (**2**) compared with the parent species (i.e., **1Me**), whereas the singlet-triplet

Table 3.2.6: PBE0/6-31+G* calculated values of hydrogenation energies (E_{hydro} , in kcal mol⁻¹) for molecules **1–6**.

Molecule	R/R'	E_{hydro}	Molecule	R/R'	E_{hydro}
1	CH ₃	2.7	4	PMe ₃	-24.3
	NMe ₂	14.0		P ⁱ Pr ₃	-20.0
	N ⁱ Pr ₂	7.1		5	CH ₃
	PMe ₂	-2.5	NMe ₂		-50.0
		P ⁱ Pr ₂	-2.9	N ⁱ Pr ₂	-49.7
2	PMe ₃	-27.1	PMe ₂	-63.2	
	P ⁱ Pr ₃	-20.2	P ⁱ Pr ₂	-63.5	
3	CH ₃	-55.5	6	PMe ₃	-19.8
	NMe ₂	-44.2		P ⁱ Pr ₃	-12.8
	N ⁱ Pr ₂	-42.0	5NHC	-17.4	
	PMe ₂	-55.5	6NHC	-26.4	
		P ⁱ Pr ₂	-56.1		

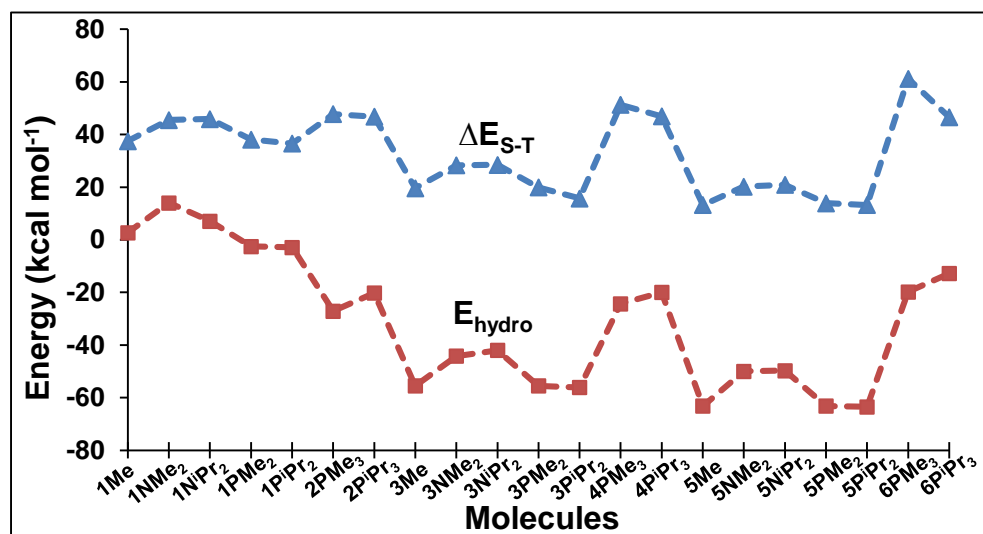


Figure 3.2.5: Graphical representation of singlet-triplet separations ($\Delta E_{\text{S-T}}$, kcal mol⁻¹) and hydrogenation energies (E_{hydro} , kcal mol⁻¹) of rNHCs **1–6**.

gaps indicate a higher stability for the same molecules. However, for the six-membered species, the hydrogenation energies show parallel behavior with that of the $\Delta E_{\text{S-T}}$ values. Interestingly, the calculated hydrogenation energies of the ylide substituted rNHCs (**2**, **4** and **6**) are found to be comparable to those of the experimentally known NHCs (**5NHC** and **6NHC**, Table 3.2.6).

The stability of a carbene can also be probed by checking its susceptibility to undergo dimerization. While carbenes with larger values of ΔE_{S-T} do not undergo dimerization, non-stabilized ones tend to undergo the same [46,51]. We have calculated the dimerization reaction energies (ΔE_{dimer}) and dimerization Gibbs free energies (ΔG_{dimer}) of some representative molecules (Table 3.2.7) and found that steric bulk plays an important role in stabilizing the singlet ground state. The dimerization is found to be disfavored (as ΔG_{dimer} becomes less negative) with an increase in the steric bulk of the substituents at position α to the carbene center. In agreement with earlier studies [50], carbenes with larger singlet-triplet separations are found to have less negative value of ΔG_{dimer} implying their likely existence as monomeric species (Table 3.2.2 and Table 3.2.7). Thus, we envisage that it may be possible to stabilize singlet rNHCs in their monomeric form by employing proper steric bulk near the carbene carbon atom.

Table 3.2.7: PBE0/6-31+G* calculated dimerization reaction energies (ΔE_{dimer} , in kcal mol⁻¹) and dimerization Gibbs free energies (ΔG_{dimer} , kcal mol⁻¹) of some representative molecules.

Molecule	ΔE_{dimer}	ΔG_{dimer}
1Me	-37.2	-23.9
1NMe₂	-13.8	0.9
1NⁱPr₂	25.5	44.5
2PMe₃	-32.1, -34.5 ^a	-12.6
2PⁱPr₃	36.8 ^b	-
3Me	-69.0	-54.5
3NMe₂	-44.4	-27.6
3NⁱPr₂	-8.3	13.8

^aThis value is without zero-point energy corrections.

^bThis value is without zero-point energy corrections. The frequency calculation of the dimer of **2PⁱPr₃** with more than 1200 basis functions is beyond our computational resources and hence, we could not provide zero-point energy corrected value for this molecule.

[3.2.3.5] Ligand Properties

Both theoretical and experimental studies have reported the superior σ -donation ability of rNHCs compared to the classical ones [43]. We have determined the energies of the σ -symmetric lone pair orbital concentrated at C_C to predict the σ -basicity of all the rNHCs and the values are listed in Table 3.2.8. Inspection of the frontier molecular

Table 3.2.8: PBE0/6-31+G* calculated energies of the σ -symmetric lone pair orbital (E_σ , in eV) concentrated at the carbene carbon of molecules **1–6**.^a

Molecule	R/R'	E_σ	Molecule	R/R'	E_σ	
1	CH ₃	-4.6	4	PMe ₃	-4.0	
	NMe ₂	-4.9		P ⁱ Pr ₃	-3.9	
	N ⁱ Pr ₂	-4.8		5	CH ₃	-5.4
	PMe ₂	-5.0			NMe ₂	-5.0
	P ⁱ Pr ₂	-4.9			N ⁱ Pr ₂	-4.8
2	PMe ₃	-4.7	PMe ₂	-5.5		
	P ⁱ Pr ₃	-4.6	P ⁱ Pr ₂	-5.5		
3	CH ₃	-4.5	6	PMe ₃	-4.1	
	NMe ₂	-4.5		P ⁱ Pr ₃	-4.0	
	N ⁱ Pr ₂	-4.3	5NHC	-6.1		
	PMe ₂	-4.8	6NHC	-5.4		
	P ⁱ Pr ₂	-4.7				

^aValues for five and six-membered normal NHCs calculated at the same level of theory are adopted from reference [28a].

orbitals show that except for the ylide-substituted ones (**2**, **4** and **6**), for all other rNHCs, the σ -symmetric lone pair orbital is represented by the HOMO whereas HOMO-1 represents the same for the former ones. The E_σ value of **1Me** is significantly higher than that of its normal counterpart **5NHC**. This is in accordance with better σ -donation ability of rNHCs compared to normal NHCs [43]. The σ -donor abilities of the five-membered rNHCs (**1** and **2**) are comparable. For the six-membered ones, the ylide substituted molecules (**4** and **6**) are significantly more electron donating (as evident from much less negative E_σ values) than others. A comparison of the E_σ value of **6NHC** with that of **3–6** indicates that except for **5**, all other six-membered rNHCs have significantly enhanced σ -donation ability than **6NHC**.

To get a quantitative measure of ylide substitution on the electron donation ability of the rNHCs under consideration, we have optimized square planar [Rh(CO)₂Cl] complexes of **1Me**, **2PMe₃**, **3Me**, **4PMe₃**, **5Me** and **6PMe₃** with the two carbonyl groups in *cis* positions as representative case. We obtained two ν_{CO} values, which appear at an average difference of ~ 80 cm⁻¹ for all these metal complexes. The lower ν_{CO} value corresponds to the asymmetric mode whereas the higher ν_{CO} value corresponds to the

symmetric stretching mode of the two carbonyl groups with respect to each other. Therefore, we have calculated the average carbonyl stretching frequencies [$\nu_{\text{CO(avg)}}$, in cm^{-1}] to get a measure of the relative electron donation abilities of the aforementioned rNHCs. The computed values for both symmetric and asymmetric as well as the average CO stretching frequencies are given in Table 3.2.9. For the six-membered carbenes, in agreement with their relative σ -donation abilities, the $\nu_{\text{CO(avg)}}$ values of the ylide-containing rNHCs (**4PMe₃** and **6PMe₃**) are significantly lower than that for the parent ones (**3Me** and **5Me**) implying greater electron donation abilities of the ylide substituted rNHCs. However, even though the E_{σ} values are comparable, the $\nu_{\text{CO(avg)}}$ value for **2PMe₃** is found to be lower than that for **1Me**.

Table 3.2.9: PBE0/6-31+G* calculated energies of the σ -symmetric lone pair orbital (E_{σ} , in eV) concentrated at the carbene carbon, carbonyl stretching frequencies (ν_{CO} in cm^{-1}) for both symmetrical and unsymmetrical stretching mode and average carbonyl stretching frequencies ($\nu_{\text{CO(avg)}}$, in cm^{-1}) of some representative L-Rh(CO)₂Cl (L = **1Me**, **2PMe₃**, **3Me**, **4PMe₃**, **5Me**, **6PMe₃**) complexes.

Molecule	E_{σ}	ν_{CO}		$\nu_{\text{CO(avg)}}$
		Unsymmetrical	Symmetrical	
1Me	-4.6	2079.9	2159.7	2119.8
2PMe₃	-4.7	2075.5	2152.7	2114.1
3Me	-4.5	2085.2	2164.1	2124.6
4PMe₃	-4.0	2081.1	2149.6	2115.3
5Me	-5.4	2096.4	2173.6	2135.0
6PMe₃	-4.1	2059.4	2151.4	2105.4

We have also calculated the values of nucleophilicity indices (N) of all the rNHCs with the help of equation $N=E_{\text{HOMO}}-E_{\text{HOMO(TCNE)}}$, considering tetracyanoethylene as the reference [38] and the values are given in Table 3.2.10. The computed values of N for all the molecules (except **2PMe₃** and **2PⁱPr₃**) are in accordance with their respective E_{σ} values. The higher basicity of rNHC **1Me** than its normal counterpart **5NHC** is also evident from the calculated nucleophilicity index value. The N values of the ylide-containing molecules (**2PMe₃** and **2PⁱPr₃**) are significantly higher than the others, whereas their E_{σ} values are same as the parent species. The origin of such discrepancy lies in the fact that E_{σ} represents the energy of the σ -symmetric lone pair orbital (which

may or may not be HOMO) whereas the nucleophilicity indices are calculated using the energies of HOMO. We obtained an excellent correlation ($R^2 = 0.96$, omitting the points corresponding to **2**, Figure 3.2.6) between the E_σ and N values.

Table 3.2.10: PBE0/6-31+G* calculated nucleophilicity index values of molecules **1–6**.^a

Molecule	R/R'	N	Molecule	R/R'	N
1	CH ₃	5.0	4	PMe ₃	5.8
	NMe ₂	4.7		P ⁱ Pr ₃	5.9
	N ⁱ Pr ₂	4.8	5	CH ₃	4.3
	PMe ₂	4.6		NMe ₂	4.6
	P ⁱ Pr ₂	4.7		N ⁱ Pr ₂	4.8
2	PMe ₃	6.1	PMe ₂	4.1	
	P ⁱ Pr ₃	6.1	P ⁱ Pr ₂	4.1	
3	CH ₃	5.1	6	PMe ₃	5.8
	NMe ₂	5.1		P ⁱ Pr ₃	6.1
	N ⁱ Pr ₂	5.3	5NHC	3.6	
	PMe ₂	4.8	6NHC	4.2	
	P ⁱ Pr ₂	4.9			

^aValues for five and six-membered normal NHCs calculated at the same level of theory are adopted from reference [28a].

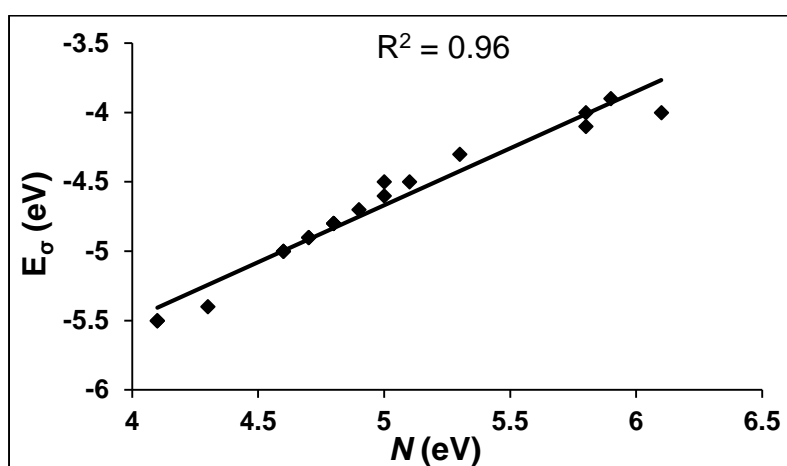


Figure 3.2.6: Correlation plot between energies of the σ -symmetric lone pair orbitals (E_σ , in eV) concentrated at the carbene carbon and nucleophilicity index (N) values for rNHCs **1** and **3–6**.

[3.2.4] Conclusions

An effort was made to stabilize remote *N*-heterocyclic carbenes (rNHCs) in their singlet state with the help of density functional theory calculations. The computed singlet-triplet gaps (ΔE_{S-T}) and hydrogenation energies (E_{hydro}) provide encouraging leads toward the possibility of realization of a metal-free remote carbene. In particular, the ylide-substituted examples are found to have large singlet-triplet gaps which fall within the range of experimentally known carbenes thereby making them suitable candidates for possible experimental realization. The presence and extent of cyclic electron delocalization in these ring systems were evaluated with the help of NICS and QTAIM calculations.

[3.3] Bibliography

- [1] (a) Balasubramanian, K. and McLean, A. D. The Singlet–Triplet Energy Separation in Silylene. *The Journal of Chemical Physics*, 85(9):5117-5119, 1986. (b) Allen, W. D. and Schaefer III, H. F. Geometrical Structures, Force Constants, and Vibrational Spectra of SiH, SiH₂, SiH₃, and SiH₄. *Chemical Physics*, 108(2):243-274, 1986.
- [2] Arduengo III, A. J., Harlow, R. L., and Kline, M. A Stable Crystalline Carbene. *Journal of the American Chemical Society*, 113(1):361-363, 1991.
- [3] Herrmann, W. A., Elison, M., Fischer, J., Köcher, C., and Artus, G. R. J. Metal Complexes of N-Heterocyclic Carbenes—A New Structural Principle for Catalysts in Homogeneous Catalysis. *Angewandte Chemie International Edition*, 34(21):2371-2374, 1995.
- [4] Enders, D., Niemeier, O., and Henseler, A. Organocatalysis by N-Heterocyclic Carbenes. *Chemical Reviews*, 107(12):5606-5655, 2007.
- [5] Hahn, F. E. and Jahnke, M. C. Heterocyclic Carbenes: Synthesis and Coordination Chemistry. *Angewandte Chemie International Edition*, 47(17):3122-3172, 2008.
- [6] Díez-González, S., Marion, N., and Nolan, S. P. N-Heterocyclic Carbenes in Late Transition Metal Catalysis. *Chemical Reviews*, 109(8):3612-3676, 2009.
- [7] Ranganath, K. V., Kloesges, J., Schäfer, A. H., and Glorius, F. Asymmetric Nanocatalysis: N-Heterocyclic Carbenes as Chiral Modifiers of Fe₃O₄/Pd Nanoparticles. *Angewandte Chemie International Edition*, 49(42):7786-7789, 2010.
- [8] Hopkinson, M. N., Richter, C., Schedler, M., and Glorius, F. An Overview of N-Heterocyclic Carbenes. *Nature*, 510(7506):485, 2014.
- [9] Arduengo III, A. J., Dias, H. R., Harlow, R. L., and Kline, M. Electronic Stabilization of Nucleophilic Carbenes. *Journal of the American Chemical Society*, 114(14):5530-5534, 1992.
- [10] Arduengo III, A. J., Goerlich, J. R., and Marshall, W. J. A Stable Thiazol-2-ylidene and Its Dimer. *European Journal of Organic Chemistry*, 1997(2):365-374, 1997.

- [11] Martin, D., Baceiredo, A., Gornitzka, H., Schoeller, W. W., and Bertrand, G. A Stable P-Heterocyclic Carbene. *Angewandte Chemie International Edition*, 44(11):1700-1703, 2005.
- [12] (a) Bourissou, D., Guerret, O., Gabbai, F. P., and Bertrand, G. Stable Carbenes. *Chemical Reviews*, 100(1):39-92, 2000. (b) Gronert, S., Keeffe, J. R., and O'Ferrall, R. A. M. Stabilities of Carbenes: Independent Measures for Singlets and Triplets. *Journal of the American Chemical Society*, 133(10):3381-3389, 2011. (c) Iversen, K. J., Wilson, D. J., and Dutton, J. L. A Computational Study on a Strategy for Isolating a Stable Cyclopentadienyl Cation. *Chemistry-A European Journal*, 20(43):14132-14138, 2014. (d) Field-Theodore, T. E., Wilson, D. J., and Dutton, J. L. Computational Predictions of the Beryllium Analogue of Borole, Cp^+ , and the Fluorenyl Cation: Highly Stabilized, Non-Lewis Acidic Antiaromatic Ring Systems. *Inorganic Chemistry*, 54(16):8035-8041, 2015.
- [13] Lavallo, V., Canac, Y., Donnadiou, B., Schoeller, W. W., and Bertrand, G. Cyclopropenylidenes: From Interstellar Space to an Isolated Derivative in the Laboratory. *Science*, 312(5774):722-724, 2006.
- [14] (a) Boehme, C. and Frenking, G. Electronic Structure of Stable Carbenes, Silylenes, and Germylenes. *Journal of the American Chemical Society*, 118(8):2039-2046, 1996. (b) Tukov, A. A., Normand, A. T., and Nechaev, M. S. N-Heterocyclic Carbenes Bearing Two, One and No Nitrogen Atoms at the Ylidene Carbon: Insight from Theoretical Calculations. *Dalton Transactions*, 2009(35):7015-7028, 2009. (c) Bazinet, P., Yap, G. P., and Richeson, D. S. Constructing a Stable Carbene with a Novel Topology and Electronic Framework. *Journal of the American Chemical Society*, 125(44):13314-13315, 2003. (d) Kuhn, N. and Al-Sheikh, A. 2, 3-Dihydroimidazol-2-Ylidenes and Their Main Group Element Chemistry. *Coordination Chemistry Reviews*, 249(7-8):829-857, 2005. (e) Nair, V., Bindu, S., and Sreekumar, V. N-Heterocyclic Carbenes: Reagents, Not Just Ligands!. *Angewandte Chemie International Edition*, 43(39):5130-5135, 2004.
- [15] (a) Alcarazo, M., Stork, T., Anoop, A., Thiel, W., and Fürstner, A. Steering the Surprisingly Modular π -Acceptor Properties of N-Heterocyclic Carbenes: Implications for Gold Catalysis. *Angewandte Chemie International Edition*, 49(14):2542-2546, 2010.

(b) Seo, H., Roberts, B. P., Abboud, K. A., Merz Jr, K. M., and Hong, S. Novel Acyclic Diaminocarbene Ligands with Increased Steric Demand and Their Application In Gold Catalysis. *Organic Letters*, 12(21):4860-4863, 2010. (c) Hudnall, T. W. and Bielawski, C. W. An N, N'-Diamidocarbene: Studies in C-H Insertion, Reversible Carbonylation, and Transition-Metal Coordination Chemistry. *Journal of the American Chemical Society*, 131(44):16039-16041, 2009. (d) Tonner, R., Heydenrych, G., and Frenking, G. Bonding Analysis of N-Heterocyclic Carbene Tautomers and Phosphine Ligands in Transition-Metal Complexes: A Theoretical Study. *Chemistry-An Asian Journal*, 2(12):1555-1567, 2007.

[16] (a) Scholl, M., Ding, S., Lee, C. W., and Grubbs, R. H. Synthesis and Activity of a New Generation of Ruthenium-Based Olefin Metathesis Catalysts Coordinated with 1, 3-Dimesityl-4, 5-Dihydroimidazol-2-Ylidene Ligands. *Organic Letters*, 1(6):953-956, 1999. (b) Trnka, T. M. and Grubbs, R. H. The Development of L₂X₂RuCHR Olefin Metathesis Catalysts: an Organometallic Success Story. *Accounts of Chemical Research*, 34(1):18-29, 2001.

[17] Huang, J., Stevens, E. D., Nolan, S. P., and Petersen, J. L. Olefin Metathesis-Active Ruthenium Complexes Bearing a Nucleophilic Carbene Ligand. *Journal of the American Chemical Society*, 121(12):2674-2678, 1999.

[18] (a) Lavallo, V., Canac, Y., Präsang, C., Donnadiu, B., and Bertrand, G. Stable Cyclic(Alkyl)(Amino)Carbenes as Rigid or Flexible, Bulky, Electron-Rich Ligands for Transition-Metal Catalysts: A Quaternary Carbon Atom Makes the Difference. *Angewandte Chemie International Edition*, 44(35), 5705-5709, 2005. (b) Lavallo, V., Canac, Y., DeHope, A., Donnadiu, B., and Bertrand, G. A Rigid Cyclic (Alkyl)(Amino) Carbene Ligand Leads to Isolation of Low-Coordinate Transition-Metal Complexes. *Angewandte Chemie International Edition*, 44(44), 7236-7239, 2005.

[19] Soleilhavoup, M. and Bertrand, G. Cyclic(Alkyl)(Amino)Carbenes (CAACs): Stable Carbenes on the Rise. *Accounts of Chemical Research*, 48(2):256-266, 2014 and references therein.

[20] Holzmann, N., Andrada, D. M., and Frenking, G. (2015). Bonding Situation in Silicon Complexes $[(L)_2(Si_2)]$ and $[(L)_2(Si)]$ with NHC and cAAC Ligands. *Journal of Organometallic Chemistry*, 792:139-148, 2015.

[21] (a) Lavallo, V., Frey, G. D., Kousar, S., Donnadiou, B., and Bertrand, G. Allene Formation by Gold Catalyzed Cross-Coupling of Masked Carbenes and Vinylidenes. *Proceedings of the National Academy of Sciences*, 104(34):13569-13573, 2007. (b) Frey, G. D., Lavallo, V., Donnadiou, B., Schoeller, W. W., and Bertrand, G. Facile Splitting of Hydrogen and Ammonia by Nucleophilic Activation at a Single Carbon Center. *Science*, 316(5823):439-441, 2007.

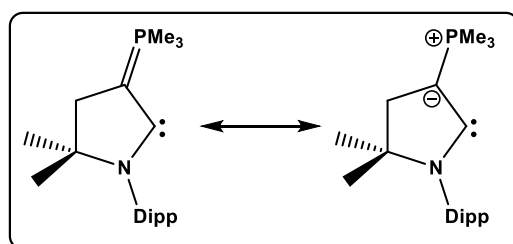
[22] Samuel, P. P., Mondal, K. C., Roesky, H. W., Hermann, M., Frenking, G., Demeshko, S., Meyer, F., Stückl, A. C., Christian, J. H., Dalal, N. S., Ungur, L., Chibotaru, L. F., Pröpper, K., Meents, A., and Dittrich, Synthesis and Characterization of a Two-Coordinate Manganese Complex and its Reaction with Molecular Hydrogen at Room Temperature. *Angewandte Chemie International Edition*, 52(45), 11817-11821, 2013.

[23] (a) Masuda, J. D., Schoeller, W. W., Donnadiou, B., and Bertrand, G. Carbene Activation of P_4 and Subsequent Derivatization. *Angewandte Chemie International Edition*, 46(37):7052-7055, 2007. (b) Masuda, J. D., Schoeller, W. W., Donnadiou, B., and Bertrand, G. NHC-Mediated Aggregation of P_4 : Isolation of a P_{12} Cluster. *Journal of the American Chemical Society*, 129(46):14180-14181, 2007. (c) Back, O., Kuchenbeiser, G., Donnadiou, B., and Bertrand, G. Nonmetal-Mediated Fragmentation of P_4 : Isolation of P_1 and P_2 Bis(carbene) Adducts. *Angewandte Chemie International Edition*, 48(30):5530-5533, 2009.

[24] (a) Nakafuji, S. Y., Kobayashi, J., and Kawashima, T. Generation and Coordinating Properties of a Carbene Bearing a Phosphorus Ylide: An Intensely Electron-Donating Ligand. *Angewandte Chemie International Edition*, 47(6):1141-1144, 2008. (b) Fürstner, A., Alcarazo, M., Radkowski, K., and Lehmann, C. W. Carbenes Stabilized by Ylides: Pushing the Limits. *Angewandte Chemie International Edition*, 47(43):8302-8306, 2008. (c) Kobayashi, J., Nakafuji, S. Y., Yatabe, A., and Kawashima, T. A Novel Ylide-Stabilized Carbene; Formation and Electron Donating Ability of an Amino(Sulfur-Ylide)Carbene. *Chemical Communications*, 2008(46):6233-6235, 2008. (d) Asay, M.,

Donnadieu, B., Baceiredo, A., Soleilhavoup, M., and Bertrand, G. Cyclic (Amino)[bis(Ylide)] Carbene as an Anionic Bidentate Ligand for Transition-Metal Complexes. *Inorganic chemistry*, 47(10):3949-3951, 2008.

[25] The ylide-stabilized carbenes can be depicted by a resonance structure consisting of a double-bonded form, as shown in Scheme 3.1.1, and a zwitterionic form, in which positive and negative charges are placed at the phosphorus and carbon atoms, respectively. An example is shown below:



[26] (a) Perdew, J. P., Burke, K., and Ernzerhof, M. Generalized Gradient Approximation Made Simple. *Physical Review Letters*, 77(18):3865, 1996. (b) Perdew, J. P., Burke, K., and Ernzerhof, M. Generalized Gradient Approximation Made Simple. *Physical Review Letters*, 78(7):1396, 1997. (c) Perdew, J. P., Ernzerhof, M., and Burke, K. Rationale for Mixing Exact Exchange with Density Functional Approximations. *The Journal of Chemical Physics*, 105(22):9982-9985, 1996. (d) Ernzerhof, M. and Scuseria, G. E. Assessment of the Perdew–Burke–Ernzerhof Exchange–Correlation Functional. *The Journal of Chemical Physics*, 110(11):5029-5036, 1999.

[27] (a) Francl, M. M., Pietro, W. J., Hehre, W. J., Binkley, J. S., Gordon, M. S., DeFrees, D. J., and Pople, J. A. Self-Consistent Molecular Orbital Methods. XXIII. A Polarization-Type Basis Set for Second-Row Elements. *The Journal of Chemical Physics*, 77(7):3654-3665, 1982. (b) Rassolov, V. A., Pople, J. A., Ratner, M. A., and Windus, T. L. 6-31G* Basis Set for Atoms K Through Zn. *The Journal of Chemical Physics*, 109(4):1223-1229, 1998. (c) Rassolov, V. A., Ratner, M. A., Pople, J. A., Redfern, P. C., and Curtiss, L. A. 6-31G* Basis Set for Third-Row Atoms. *Journal of Computational Chemistry*, 22(9):976-984, 2001. (d) Dolg, M., Wedig, U., Stoll, H., and Preuss, H. Energy-Adjusted Abinitio Pseudopotentials for the First Row Transition Elements. *The Journal of Chemical Physics*, 86(2):866-872, 1987. (e) Andrae, D., Haeussermann, U., Dolg, M., Stoll, H., and Preuss, H. Energy-Adjusted Abinitio

Pseudopotentials for the Second and Third Row Transition Elements. *Theoretica Chimica Acta*, 77(2):123-141, 1990. (f) Alkauskas, A., Baratoff, A., and Bruder, C. Gaussian Form of Effective Core Potential and Response Function Basis Set Derived from Troullier–Martins Pseudopotential: Results for Ag and Au. *The Journal of Physical Chemistry A*, 108(33):6863-6868, 2004.

[28] (a) Phukan, A. K., Guha, A. K., Sarmah, S., and Dewhurst, R. D. Electronic and Ligand Properties of Annelated Normal and Abnormal (Mesoionic) N-Heterocyclic Carbenes: a Theoretical Study. *The Journal of Organic Chemistry*, 78(21):11032-11039, 2013. (b) Phukan, A. K., Guha, A. K., and Sarmah, S. Ligand Properties of Boron-Substituted Five-, Six-, and Seven-Membered Heterocyclic Carbenes: a Theoretical Study. *Organometallics*, 32(11):3238-3248, 2013. (c) Guha, A. K. and Phukan, A. K. Theoretical Study on the Effect of Annelation and Carbonylation on the Electronic and Ligand Properties of N-Heterocyclic Silylenes and Germylenes: Carbene Comparisons begin To Break Down. *The Journal of Organic Chemistry*, 79(9):3830-3837, 2014. (d) Borthakur, B., Rahman, T., and Phukan, A. K. Tuning the Electronic and Ligand Properties of Remote Carbenes: A Theoretical Study. *The Journal of Organic Chemistry*, 79(22):10801-10810, 2014.

[29] (a) Fokin, A. A., Chernish, L. V., Gunchenko, P. A., Tikhonchuk, E. Y., Hausmann, H., Serafin, M., Dahl, J. E. P., Carlson R. M. K., and Schreiner, P. R. Stable Alkanes Containing Very Long Carbon–Carbon Bonds. *Journal of the American Chemical Society*, 134(33):13641-13650, 2012. (b) Rekker, B. D., Brown, T. M., Fettinger, J. C., Lips, F., Tuononen, H. M., Herber, R. H., and Power, P. P. Dispersion Forces and Counterintuitive Steric Effects in Main Group Molecules: Heavier Group 14 (Si–Pb) Dichalcogenolate Carbene Analogues with Sub-90° Interligand Bond Angles. *Journal of the American Chemical Society*, 135(27):10134-10148, 2013. (c) Hering, C., Schulz, A., and Villinger, A. Low-Temperature Isolation of An Azidophosphenium Cation. *Angewandte Chemie International Edition*, 51(25):6241-6245, 2012.

[30] Iglesias, M., Beetstra, D. J., Knight, J. C., Ooi, L. L., Stasch, A., Coles, S., Male, L., Hursthouse, M. B., Cavel, K. J., Dervisi, A., and Fallis, I. A. Novel Expanded Ring N-Heterocyclic Carbenes: Free Carbenes, Silver Complexes, and Structures. *Organometallics*, 27(13):3279-3289, 2008.

[31] Krahulic, K. E., Enright, G. D., Parvez, M., and Roesler, R. A Stable N-Heterocyclic Carbene with a Diboron Backbone. *Journal of the American Chemical Society*, 127(12):4142-4143, 2005.

[32] Präsang, C., Donnadiou, B., and Bertrand, G. Stable Planar Six- π -Electron Six-Membered N-Heterocyclic Carbenes with Tunable Electronic Properties. *Journal of the American Chemical Society*, 127(29):10182-10183, 2005.

[33] (a) Glendening, E. D., Reed, A. E., Carpenter, J. E., and Weinhold, F. NBO Program, Version 3.1; University of Wisconsin: Madison, WI, 1988. (b) Reed, A. E., Curtiss, L. A., and Weinhold, F. Intermolecular Interactions from a Natural Bond Orbital, Donor-Acceptor Viewpoint. *Chemical Reviews*, 88(6):899-926, 1988.

[34] Frisch, M. J., Trucks, G. W., Schlegel, H. B., Scuseria, G. E., Robb, M. A., Cheeseman, J. R., Montgomery, J. A., Jr., Vreven, T., Kudin, K. N., Burant, J. C., Millam, J. M., Iyengar, S. S., Tomasi, J., Barone, V., Mennucci, B., Cossi, M., Scalmani, G., Rega, N., Petersson, G. A., Nakatsuji, H., Hada, M., Ehara, M., Toyota, K., Fukuda, R., Hasegawa, J., Ishida, M., Nakajima, T., Honda, Y., Kitao, O., Nakai, H., Klene, M., Li, X., Knox, J. E., Hratchian, H. P., Cross, J. B., Bakken, V., Adamo, C., Jaramillo, J., Gomperts, R., Stratmann, R. E., Yazyev, O., Austin, A. J., Cammi, R., Pomelli, C., Ochterski, J. W., Ayala, P. Y., Morokuma, K., Voth, G. A., Salvador, P. J., Dannenberg, J., Zakrzewski, V. G., Dapprich, S., Daniels, A. D., Strain, M. C., Farkas, O., Malick, D. K., Rabuck, A. D., Raghavachari, K., Foresman, J. B., Ortiz, J. V., Cui, Q., Baboul, A. G., Clifford, S., Cioslowski, J., Stefanov, B. B., Liu, G., Liashenko, A., Piskorz, P., Komaromi, I., Martin, R. L., Fox, D. J., Keith, T., Al-Laham, M. A., Peng, C. Y., Nanayakkara, A., Challacombe, M., Gill, P. M. W., Johnson, B., Chen, W., Wong, M. W., Gonzalez, C., and Pople, J. A. *Gaussian 03, Revision D.02*; Gaussian, Inc., Pittsburgh, PA, 2003.

[35] (a) Jacobsen, H., Correa, A., Poater, A., Costabile, C., and Cavallo, L. Understanding the M-(NHC) (NHC= N-heterocyclic carbene) bond. *Coordination Chemistry Reviews*, 253(5-6):687-703, 2009. (b) Radius, U. and Bickelhaupt, F. M. Bonding Capabilities of Imidazol-2-Ylidene Ligands in Group-10 Transition-Metal Chemistry. *Coordination Chemistry Reviews*, 253(5-6):678-686, 2009.

- [36] Tonner, R., Heydenrych, G., and Frenking, G. First and Second Proton Affinities of Carbon Bases. *ChemPhysChem*, 9(10):1474-1481, 2008.
- [37] (a) Chianese, A. R., Li, X., Janzen, M. C., Faller, J. W., and Crabtree, R. H. Rhodium and Iridium Complexes of N-Heterocyclic Carbenes via Transmetalation: Structure and Dynamics. *Organometallics*, 22(8):1663-1667, 2003. (b) Gusev, D. G. Donor Properties of a Series of Two-Electron Ligands. *Organometallics*, 28(3):763-770, 2009.
- [38] Domingo, L. R., Chamorro, E., and Pérez, P. Understanding the Reactivity of Captodative Ethylenes in Polar Cycloaddition Reactions. A Theoretical Study. *The Journal of Organic Chemistry*, 73(12):4615-4624, 2008.
- [39] El-Hellani, A., Monot, J., Tang, S., Guillot, R., Bour, C., and Gandon, V. Relationship Between Gallium Pyramidalization in L-GaCl₃ Complexes and the Electronic Ligand Properties. *Inorganic Chemistry*, 52(19):11493-11502, 2013.
- [40] Igau, A., Grutzmacher, H., Baceiredo, A., and Bertrand, G. Analogous α, α' -Bis-Carbenoid Triply Bonded Species: Synthesis of a Stable λ^3 -Phosphinocarbene- λ^5 -Phosphaacetylene. *Journal of the American Chemical Society*, 110(19):6463-6466, 1988.
- [41] Schuster, O., Yang, L., Raubenheimer, H. G., and Albrecht, M. Beyond Conventional N-Heterocyclic Carbenes: Abnormal, Remote, and Other Classes of NHC Ligands with Reduced Heteroatom Stabilization. *Chemical Reviews*, 109(8):3445-3478, 2009.
- [42] (a) Han, Y. and Huynh, H. V. Preparation and Characterization of the First Pyrazole-Based Remote N-Heterocyclic Carbene Complexes of Palladium(II). *Chemical Communications*, 2007(10):1089-1091, 2007. (b) Schneider, S. K., Rentzsch, C. F., Krüger, A., Raubenheimer, H. G., and Herrmann, W. A. Pyridin- and Quinolinylidene Nickel Carbene Complexes as Effective Catalysts for the Grignard Cross-Coupling Reaction. *Journal of Molecular Catalysis A: Chemical*, 265(1-2):50-58, 2007.
- [43] (a) Schneider, S. K., Roembke, P., Julius, G. R., Loschen, C., Raubenheimer, H. G., Frenking, G., and Herrmann, W. A. Extending the NHC Concept: C-C Coupling Catalysis by a Pd(II) Carbene (rNHC) Complex with Remote Heteroatoms. *European Journal of Inorganic Chemistry*, 2005(15):2973-2977, 2005. (b) Schneider, S. K., Julius,

G. R., Loschen, C., Raubenheimer, H. G., Frenking, G., and Herrmann, W. A. A First Structural and Theoretical Comparison of Pyridinylidene-Type rNHC (Remote N-Heterocyclic Carbene) and NHC Complexes of Ni(II) Obtained by Oxidative Substitution. *Dalton Transactions*, 2006(9):1226-1233, 2006.

[44] Mayer, U. F., Murphy, E., Haddow, M. F., Green, M., Alder, R. W., and Wass, D. F. A New Class of Remote N-Heterocyclic Carbenes with Exceptionally Strong σ -Donor Properties: Introducing Benzo[c]quinolin-6-ylidene. *Chemistry-A European Journal*, 19(13):4287-4299, 2013.

[45] Keith, T. A. AIMAll, version 14.11.23; Available at: <http://aim.tkgristmill.com>.

[46] Melaimi, M., Soleilhavoup, M., and Bertrand, G. Stable Cyclic Carbenes and Related Species Beyond Diaminocarbenes. *Angewandte Chemie International Edition*, 49(47):8810-8849, 2010.

[47] (a) Becke, A. D. Density-Functional Thermochemistry. III. The Role of Exact Exchange. *The Journal of Chemical Physics*, 98(7):5648-5652, 1993. (b) Zhao, Y. and Truhlar, D. G. The M06 Suite of Density Functionals for Main Group Thermochemistry, Thermochemical Kinetics, Noncovalent Interactions, Excited States, and Transition Elements: Two New Functionals and Systematic Testing of Four M06-Class Functionals and 12 Other Functionals. *Theoretical Chemistry Accounts*, 120(1-3):215-241, 2008. (c) Krishnan, R., Binkley, J. S., Seeger, R., and Pople, J. A. Self-Consistent Molecular Orbital Methods. XX. A Basis Set for Correlated Wave Functions. *The Journal of Chemical Physics*, 72(1):650-654, 1980. (d) McLean, A. D. and Chandler, G. S. Contracted Gaussian Basis Sets for Molecular Calculations. I. Second Row Atoms, Z=11-18. *The Journal of Chemical Physics*, 72(10):5639-5648, 1980.

[48] Schleyer, P. v. R., Maerker, C., Dransfeld, A., Jiao, H., and Hommes, N. J. R. v. E. Nucleus-Independent Chemical Shifts: A Simple and Efficient Aromaticity Probe. *Journal of the American Chemical Society*, 118(26):6317-6318, 1996.

[49] Williams, R. V. Homoaromaticity. *Chemical Reviews*, 101(5):1185-1204, 2001.

[50] (a) Bader, R. F. A Quantum Theory of Molecular Structure and its Applications. *Chemical Reviews*, 91(5):893-928, 1991. (b) Foroutan-Nejad, C. Interatomic

Magnetizability: a QTAIM-Based Approach Toward Deciphering Magnetic Aromaticity. *The Journal of Physical Chemistry A*, 115(45):12555-12560, 2011. (c) Velian, A. and Cummins, C. C. Synthesis and Characterization of $P_2N_3^-$: An Aromatic Ion Composed of Phosphorus and Nitrogen. *Science*, 348(6238):1001-1004, 2015.

[51] (a) Nyulászi, L., Veszprémi, T., and Forró, A. Stabilized Carbenes do not Dimerize. *Physical Chemistry Chemical Physics*, 2(14):3127-3129, 2000. (b) Vignolle, J., Cattoen, X., and Bourissou, D. Stable Noncyclic Singlet Carbenes. *Chemical Reviews*, 109(8):3333-3384, 2009. (c) Bernhammer, J. C., Frison, G., and Huynh, H. V. Electronic Structure Trends in N-Heterocyclic Carbenes (NHCs) with Varying Number of Nitrogen Atoms and NHC-Transition Metal Bond Properties. *Chemistry-A European Journal*, 19(38):12892-12905, 2013.